Potential mechanisms of calcium dependent regulation of the mammalian cell cycle revealed by comprehensive unbiased label-free nLC-MS/MS quantitative proteomics

Accepted Manuscript

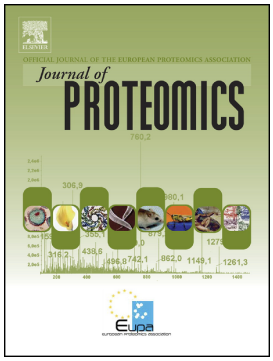

Potential mechanisms of calcium dependent regulation of the mammalian cell cycle revealed by comprehensive unbiased label-free nLC-MS/MS quantitative proteomics

Anna Kwasnik, Alex von Kriegsheim, Andrew Irving, Stephen R. Pennington

PII: S1874-3919(17)30269-5
DOI: doi: 10.1016/j.jprot.2017.08.006
Reference: JPROT 2917

To appear in: *Journal of Proteomics*

Received date: 21 November 2016
Revised date: 3 August 2017
Accepted date: 5 August 2017

Please cite this article as: Anna Kwasnik, Alex von Kriegsheim, Andrew Irving, Stephen R. Pennington , Potential mechanisms of calcium dependent regulation of the mammalian cell cycle revealed by comprehensive unbiased label-free nLC-MS/MS quantitative proteomics, *Journal of Proteomics* (2017), doi: 10.1016/j.jprot.2017.08.006

Potential mechanisms of calcium dependent regulation of the mammalian cell cycle revealed by comprehensive unbiased label-free nLC-MS/MS quantitative proteomics

Anna Kwasnik[1], Alex von Kriegsheim[1,2,3], Andrew Irving[4], Stephen R Pennington*[1]

Highlights:

- Global proteomic effect of Ca^{2+} influx inhibition on G_1 phase was examined
- A total 182 differentially expressed proteins were identified with diverse functions
- Cell proliferation, cell morphology, and cellular assembly and organisation were altered by the inhibition of Ca^{2+} influx.
- Potential mechanism of Ca^{2+} dependent regulation of cell cycle was proposed
- Selected protein expression changes and biological processes were validated.

[1] School of Medicine, Conway Institute of Biomolecular and Biomedical Research, University College Dublin, Belfield, Dublin 4, Ireland.

[2] Systems Biology Ireland, University College Dublin, Belfield, Dublin 4, Ireland

[3]Edinburgh Cancer Research Centre, Institute of Genetics and Molecular Medicine, University of Edinburgh, Western General Hospital, Crewe Road South, EH4 2XR, United Kingdom

[4] School of Biomolecular and Biomedical Sciences, Conway Institute of Biomolecular and Biomedical Research, University College Dublin, Belfield, Dublin 4, Ireland

*Corresponding author

Prof Stephen R Pennington
Professor of Proteomics
School of Medicine, UCD Conway Institute
University College Dublin
Belfield, Dublin 4, Ireland
Phone: (+353) 1 716 6783
Email: stephen.pennington@ucd.ie

Abstract

Calcium (Ca^{2+}) controls progression through the mammalian cell cycle by engaging a diverse range of molecular pathways. While the essential role of spatio-temporal Ca^{2+} signaling in the cell cycle is well established, the precise mechanisms by which it regulates cell cycle entry and progression through G_1 are not particularly well understood.

Here, high-resolution label-free semi-quantitative nLC-MS/MS analysis has been used to support a highly reproducible unbiased analysis of Ca^{2+} influx dependent growth factor induced protein expression early in G_1 in human fibroblasts. Using this strategy a panel of 182 proteins whose expression was Ca^{2+} dependent were identified. Pathway analysis has indicated that Ca^{2+} likely regulates cell proliferation via PI3K/AKT pathway and its downstream target mTOR. In addition to cell proliferation found proteins were involved in the regulation of cell morphology and cellular assembly and organization, the environmental clues, which are known to regulate G_1 progression.

Reported here data represents one of the most comprehensive proteomic datasets of growth factor and Ca^{2+} dependent protein expression in the mammalian cell cycle and provides a rich source of publically available data to support continued investigation of the role of Ca^{2+} in G_1 progression at both the molecular and systems level.

Keywords: cell cycle, G_1 phase, calcium influx, nLC-MS/MS, cell shape

Introduction

Cell division is essential for the growth, maintenance and reproduction of all mammalian organisms [1,2]. A detailed knowledge of the biochemical events that regulate the complex temporal sequence of events, which comprises the cell division is therefore central to understanding both normal physiology and disease. Notably, cancer is accompanied by aberrant regulation of the cell division cycle [3] and identification of the key regulatory biochemical events in this process provides an opportunity to develop strategies for cancer therapy [4,5].

Evidence from a number of studies, has shown that capacitive calcium entry (CCE) - also called store operated calcium entry (SOCE) - plays a fundamental role in cell cycle initiation and progression through the cell cycle in non-excitable cells including fibroblasts [6–8]. It is recognised that the transient increase in cytoplasmic levels of Ca^{2+} following growth factor stimulation of cells acts as a mitogenic signal contributing to the initiation of the G_0/G_1 transition, regulation of G_1 progression and subsequent entry into S phase [9]. The mechanism of capacitive Ca^{2+} entry (CCE), in which inositol (1,4,5) trisphosphate activated release of Ca^{2+} from internal ER stores triggers the entry of Ca^{2+} from outside the cell, was first proposed by Putney in 1986 [10]. For many years the key components involved in this coupling between store release and Ca^{2+} entry were unknown but the role of Ca^{2+} entry was investigated with some success by use of several inhibitors of CCE. Among these inhibitors is the imidazole derivative SK&F96365 and a range of reports have shown that it efficiently and reversibly blocks Ca^{2+} influx [7,11], and inhibits the proliferation of multiple cell lines [7,12–15]. Growth factors and mitogens evoke typical biphasic changes in cytoplasmic Ca^{2+} levels. Initially there is a rapid transient rise contributed by the releasing of Ca^{2+} from internal ER stores and this is followed by a sustained elevated plateau during G_1 phase

contributed by Ca^{2+} influx from external stores [9,16]. In the absence of extracellular Ca^{2+} or when Ca^{2+} influx is blocked (including by SK&F96365), mitogens evoke a transient elevation of Ca^{2+} but do not show the subsequent sustained plateau of elevated Ca^{2+} or progression to S phase [16]. In fibroblasts, the sustained plateau is mediated by Ca^{2+} influx, which is regulated by CCE. Together these observations reveal that CCE mediated Ca^{2+} influx is necessary for Ca^{2+} dependent regulation of the G_1 phase events that occur during the plateau phase and ultimately are required for progression to S phase. The discovery of two critical molecular components of CCE - STIM [17] and Orai [18] proteins – has provided additional evidence that Ca^{2+} influx is necessary for the proliferation of both normal and cancer cell lines [19–22].

Despite the role of Ca^{2+} in regulation of the cell cycle being well established and there being much known about the biochemical events that regulate G_1 phase progression, the molecular mechanism(s) by which Ca^{2+} signalling regulates these G_1 biochemical events is poorly characterised [23,24]. Notably, when quiescent cells (in G_0) are exposed to growth factors and mitogens a series of intracellular signalling events are initiated to control entry into and progression through G_1 phase. These signals include the activation of receptor tyrosine kinases (RTK) and engagement of multiple signalling pathways, including the mitogen-activated protein kinase (MAPK) pathway. Importantly, Katoch *et al.* have shown that the activity of ERK1/ERK2 - components of the MAPK pathway - is Ca^{2+} dependent [25]. The downstream targets of the mitogen signalling pathways and the key proteins that regulate G_1 progression are cyclin dependent kinases (CDK; CDK4/6 and CDK2) and cyclins D and E [26]. The expression of D and E type cyclins is positively regulated by ERK1/ERK2 through the regulation of transcription factors such as NF-κB, AP-1, STAT or CREB. Importantly it has been shown that Ca^{2+} dependent regulation of ERK1/ERK2 inhibits cyclin

D1 transcription through NF-κB [27]. There is also indication that Ca^{2+} is important for the expression of the immediate-early genes including *FOS*, *JUN* and *MYC* [28–30].

Evidence from multiple studies directly (deletion of components of CCE, STIM and ORAI) or indirectly (blocking with specific inhibitors) targeting CCE, have confirmed that Ca^{2+} controls the transition of cells through the R point by regulating the expression and function of key G_1 phase regulatory proteins such as CDK and their associated activating cyclins and cyclin dependent kinases inhibitors [30–32]. Furthermore, Ca^{2+} is required for retinoblastoma (Rb) phosphorylation [28,30,33].

In an early study to investigate the effect of Ca^{2+} influx on gene and protein expression induced by growth factor we showed that treatment of murine fibroblasts with SK&F96365 regulated multiple genes at the both transcript and protein level [12]. Here, we used biological replicate, rigorous sample preparation and high resolution mass spectrometry to establish at a comprehensive level the extent to which growth factor induced changes in protein expression are dependent on Ca^{2+} influx. Out of 4,411 proteins identified by nLC-MS/MS analysis across all conditions, the expression of 182 proteins was influenced by inhibition of Ca^{2+} influx. We have used pathway analysis to attempt to reveal which of these Ca^{2+} sensitive proteins may regulate cell proliferation. Notably, we have identified a panel of proteins including ACP1, CDC42, EGFR, F2R, ERBB4, HRAS, IKBKB, PIK3R1, PAX and RHOB. that are known to be involved in both cell proliferation and cell morphology (which is influenced by Ca^{2+} influx). These proteins represent key targets for further mechanistic studies to investigate how Ca^{2+} signalling and the regulation of cell shape may control the progression of mammalian cells through G_1 to S phase including via one mechanism proposed here.

EXPERIMENTAL SECTION

Cell Culture

Human MRC-5 cells were grown in MEM (Minimum Essential Medium Eagle (MEM; Sigma-Aldrich) supplemented with 10 mM L-glutamine, 5 mM sodium pyruvate, MEM non-essential amino acid solution (Sigma-Aldrich) and 1 % penicillin/streptomycin (Life Technologies, Gibco) hereafter referred to as 'full MEM' to which was added 10 % FBS (HyClone). Cells were maintained in humidified atmosphere of 5 % CO2 at 37 °C and regularly sub-cultured with 0.25 % Trypsin – EDTA (Life Technologies, Gibco) by standard procedures.

Generation of quiescent, synchronised MRC-5 cells

Exponentially growing MRC-5 cells were sub-cultured into 6-well plates at 5 x 10^5 cells per well and incubated overnight in full MEM containing 10 % FBS to allow cell attachment. Cells were then washed 3 times in full MEM containing 0.2 % FBS and incubated for a further 24 h in the same medium (full MEM containing 0.2 % FBS) to synchronise cells in G_0/G_1.

Induction of cells to re-enter cell cycle

To induce cell cycle re-entry MRC-5 cells, were stimulated with either 10 % FBS MEM medium or MEM medium supplemented with a defined mixture of growth factors: 10 ng/ml EGF (PeproTech), 50 ng/ml dexamethasone (Sigma-Aldrich), 5 µg/ml apo-Transferrin (Sigma-Aldrich), 5 µg/ml insulin (Sigma-Aldrich) and 0.5 % albumin from bovine serum (Sigma-Aldrich), as described previously [34,35].

Cell treatment with Ca^{2+} influx inhibitor SK&F96365

A stock of 10 mM SK&F96365 (Santa Cruz Biotechnology) was prepared by dissolving SK&F96365 in DMSO (Sigma-Aldrich) and stored at -20 °C. The final concentrations of SK&F96365 used in experiments were prepared by diluting SK&F96365 stock in a medium that was used in experiments. Quiescent cells were incubated with SK&F96365 alone for 15 min prior to stimulation of cells with FBS or mixture of growth factors.

Live cell Ca2+ measurement

Cytosolic Ca^{2+} levels were estimated in live cells by the measurement of the fluorescent emission of Ca^{2+} indicator Fura-2 at two excitation maxima, 380 nm for Ca^{2+} unbound and 340 nm for Ca^{2+} bound form of Fura-2 [36]. MRC-5 cells for these experiments were seeded on 9 mm round glass cover slips that were placed in the wells of 24 well plates. Cells were seeded at 60,000 cells per well and incubated in full MEM medium containing 0.2 % FBS for 24 h. A stock of Fura-2 (Thermo Fisher Scientific) was dissolved in DMSO at concentration of 2 mM. The final, 6 µM concentration of Fura-2 was prepared by diluting Fura-2 stock in Ca^{2+} recording buffer (125 mM NaCl (Sigma-Aldrich), 2 mM $MgCl_2$ (Calbiochem®), 4.5 mM KCl (Fluka), 10 mM Glucose (Gibco®), 2 mM CaCl2 (Sigma-Aldrich) and 20 mM HEPES (Sigma-Aldrich) at pH 7.4 in presence of 0.2 % FBS). 3 µl of Fura-2 stock was re-suspended in 1 ml of Ca^{2+} recording buffer by sonication. Glass cover slips with quiescent MRC-5 cells were transferred to 35 x 10 mm EASY GRIP tissue culture dishes, washed 3 times with calcium recording buffer and then 1 ml of 6 µM Fura-2 solution was added. Cells were loaded with Fura-2 for an hour at RT protected from light. Cells were then washed three times in Ca^{2+} recording buffer and left in the same buffer for additional 20 min at RT protected from light.

Fura-2 loaded cells were incubated in 20 µM of SK&F96365 for an hour in Ca^{2+} recording buffer prior to Ca^{2+} imaging to stabilise cytoplasmic Ca^{2+} levels. Images were captured using a microscope equipped with 60X water-immersion objective and a 12-bit cooled CCD camera and capturing board (Sensicam, PCO, Germany) as described previously [37]. For excitation of Fura-2 at 340/380 nm a PolyChrome IV monochromator (Till Photonics, Germany) was used. To avoid bleaching of Fura-2 the monochromator was attenuated with neutral density filters. Detected light signals were transmitted to the computer and recorded by MetaFluor Fluorescence Ratio Imaging Software (Molecular Devices, LLC; USA). The excitation of Fura-2 was recorded in a time dependent manner and the images were acquired in a fast mode using 2×2 binning with a temporal resolution of ~100 mseconds per frame. Recorded Ca^{2+} images were analysed with MetaFluor software. Individual cells were selected by drawing a region of interest (ROI) around the cell and the Fura-2 ratio 340/380 was recorded and saved as numerical values. Each value was normalised by subtracting background noise from a cell free region. Numerical values were then exported to OrginPro 8 SR0 software (version 8.0724). Data from individual cells was plotted separately as traces and as an average of all cells analysed on one glass cover slip as a linear function of time versus Fura-2 ratio of the two fluorescent excitation wavelengths for bound and unbound Fura-2. Due to the difference in Fura-2 loading between different experimental conditions the data from control and SK&F96365 treated cells were compared by normalising data to the same values.

Measurement of cell proliferation

Proliferation of MRC-5 cells was monitored using carboxyfluorescein succinimidyl ester (CFSE), a dye that covalently binds to all free amines on the surface and inside the cell. Cell

proliferation is monitored by flow cytometry via monitoring of the fluorescent intensity of the CFSE over the period of time. A stock of CFSE (Thermo Fisher Scientific) was dissolved in DMSO at concentration of 5 mM. The final, 5 µM concentration of CFSE was prepared by diluting CFSE stock in phosphate buffered saline (PBS; OXOID). Quiescent MRC-5 cells were washed 3 times with PBS and then 1 ml of 5 µM CFSE solution was added to each well and cells were incubated with CFSE for 20 min at humidified atmosphere of 5 % CO2 at 37 °C covered with tin foil to protect from light. The CFSE staining solution was removed by aspiration and cells were washed twice in 1 % solution of albumin from bovine serum in PBS and twice in full MEM medium containing 0.2 % FBS. CFSE loaded cells were left overnight in 0.2 % FBS MEM medium. Cells were then stimulated to enter cell cycle with 10 % FBS or mixture of growth factors in the presence or absence of SK&F96365. 48 h after stimulation, cells were harvested by trypsinisation and washed once with ice-cold PBS by centrifugation for 5 min at 1,200 rpm at 4 °C. Cell pellets were then resuspended in 100 µl of PBS and analysed on an Accuri C6 flow cytometer (Becton, Dickinson and Company). The mean intensity of the CFSE dye was quantified using FCS 4 Express Flow Cytometry software, version 4.07.0020. All samples were analysed as biological triplicates.

Cell cycle analysis

Cells were harvested by trypsinisation and washed twice with PBS at 4 °C. Cells were fixed with ice cold 70 % ethanol, pelleted by centrifugation and washed twice with PBS at 4 °C. Cells were then treated with RNase A (20 µg/ml; Sigma-Aldrich) and incubated with 40 µg/ml of propidium iodide (Sigma-Aldrich) for 30 min and then analysed on an Accuri C6 flow cytometer (Becton, Dickinson and Company). DNA content was quantified using FCS 4

Express Flow Cytometry software, version 4.07.0020. All samples were analysed as biological triplicates.

Sample preparation for nLC-MS/MS

Samples were prepared according to the filter aided sample preparation (FASP) method as described by Wiśniewski *et al.* [38] . Briefly, adherent cells were washed twice with ice-cold PBS and then lysed by sonication in SDS lysis buffer (0.2 % (v/v) SDS in 0.1 M Tris/HCl, pH 7.6). Samples were heated at 95 °C for 5 min and after centrifugation of cell debris; the supernatants were assayed for protein concentration (BCA assay kit (Pierce)). Subsequently cell lysate proteins (100 µg in 100 µl) were reduced with DTT (final concentration of 0.1 M), combined with 200 µl of UA buffer (8 M urea in 0.1 M Tris/HCl, pH 8.5), loaded onto 30,000 MWCO Vivacon 500 spin membranes (Sartorius) and centrifuged at 14,000 g for 40 min. Spin filter membranes were subsequently washed with UA buffer and then bound proteins were alkylated with final concentration of 0.05 M iodoacetamide. Spin Filter membranes were then washed three times in UB buffer (8 M urea in 0.1 M Tris/HCl, pH 8.0). Proteins on the spin filters were subsequently digested with Lys-C and trypsin. Initially proteins were digested overnight with Lys-C (enzyme: substrate 1:50) and then for additional 3 h with trypsin (enzyme: substrate 1:100). Both digestions were performed at 37 °C. Digestion was stopped by the acidification of samples to a final concentration of 1 % TFA. The final concentration of peptides was estimated (NanoDrop readings at 280 nm) and prior to mass spectrometry analysis, peptides were desalted and purified with in house prepared stage tip [39,40]. Briefly, stage tips were activated by washing with 50 % ACN 0.1 % TFA prior to addition of peptides in aqueous 1 % TFA. The stage tips were then washed twice with 1 %

TFA and peptides were eluted with 50 % ACN, 0.1 % TFA and then dried by evaporation (speed vacuum).

nLC-MS/MS

Samples were analysed by nano-flow reverse phase LC using a Q-Exactive mass spectrometer connected online to an Ultimate Ultra3000 chromatography system (both Thermo Fisher Scientific) as described [41]. Briefly, dried peptides were reconstituted in 0.1 % TFA and 2 µg of each sample were loaded on in house prepared analytical column (150 mm length, 75 µm inside diameter) packed in house with 1.9 µm ReprosilAQ C18 (Dr Maisch GmbH). Tryptic peptides were separated using a 130 minute linear gradient from 4 % to 32 % acetonitrile at a flow rate of 250 nl/min. The mass spectrometer was operated in data-dependent acquisition mode with a top-12 MS/MS scanning approach. For protein label-free identification and quantification, tandem mass spectra and peptide fragments of the 12 most abundant peaks were acquired in the linear ion trap by peptide fragmentation using higher energy collisional dissociation (HID). A 2300 V potential was applied to column with a capillary temperature of 320 °C. Each biological sample was analysed as a technical duplicate. Experiments were repeated a minimum of three times.

Data processing and analysis

MS and MS/MS data were processed using MaxQuant computational proteomics platform [42,43] version 1.4.1.2. Peak lists, generated in MaxQuant were searched using Andromeda [44] peptide search engine against the UniProt database (release 2013_12, taxonomy Homo Sapiens) containing 39,648 protein entries supplemented with frequently observed contaminants and containing forward and reverse sequences. Multiplicity was set to one

and trypsin specified with up to two missed cleavages. Carbamidomethylation of cysteines was defined as a static modification, oxidation of methionine and protein N-terminal acetylation were set as variable modifications. Minimum peptide length of 7 was set and 6 ppm and 20 ppm was used for fragmented and precursor mass tolerances respectively. A retention time tolerance of 1 min was used to align any time shift in acquisition between samples. False discovery rates (FDR) at both peptide and protein levels were set at 1 %. Protein identification was performed with at least one unique peptide.

Bioinformatics analysis was performed with Perseus software. Variability between biological (n=3) and technical (n=2) replicates is reported as Pearson and r2 correlations as $\log_2$ values. Data for analysis was transformed to a $\log_2$ scale and missing values were imputed with constant values to allow the assignment of the presence or absence of proteins between conditions. All statistical Student's t-tests, to distinguish proteins differentially expressed between conditions, were performed with a p-value threshold of 0.05. For hierarchical clustering, Euclidean distances were applied using logarithmised intensities after z-score normalisation of the statistically significant data. Principal component analysis was undertaken on logarithmised values only.

Differentially expressed proteins were further analysed using Ingenuity Pathway Analysis Knowledge Database (Ingenuity Systems) to map statistically significant proteins to the pathways and biological processes in which they were enriched.

Sample Preparation for Immunoblotting

Cells were washed twice with ice-cold PBS and then lysed in RIPA buffer (Thermo Fisher Scientific) in the presence of protease (0.5 % v/v final concentration; Sigma-Aldrich) and

phosphatase inhibitors (1 % v/v final concentration; Sigma-Aldrich). Cell lysates were then transferred to Eppendorf tubes and incubated for 15 min on ice. Following this, samples were centrifuged at 18,000 g for 20 min at 4 °C and supernatants were transferred to new Eppendorf tubes.

Total protein concentration was determined using the BCA assay according to the manufacturer's instructions (Pierce). For each sample, 20 µg of total protein (in 10 µl RIPA buffer) was mixed with 10 µl of SDS sample buffer (400 mM Tris-HCl [pH 6.8], 30 % glycerol, 10 % SDS, 0.2 M DTT, 0.02 % Coomassie blue G-250) and samples were denatured by heating at 95 °C for 5 min.

Immunoblotting

Protein samples were separated by SDS-PAGE using in house made 10 or 12 % polyacrylamide gels run on Mini-PROTEAN® Tetra Handcast Systems (Bio-Rad). Denatured samples (20 µg total protein) were loaded into the wells of 4 % stacking gels using a micropipette. Electrophoresis of gels was undertaken at 100 V (constant voltage) using 0.025 M Tris, 0.192 M glycine and 1 % SDS running buffer. To determine the relative molecular weight of immunoblotted proteins, Precision Plus Protein dual colour marker (Bio-Rad) was loaded onto each gel.

Electrophoretically separated proteins were transferred onto PVDF transfer membranes (PerkinElmer), pre-soaked in 100 % methanol using a wet mini-transfer apparatus (Bio-Rad). The filter paper, sandwiching padding and gels were pre-soaked in transfer buffer (0.025 M Tris, 0.192 M glycine and 20 % methanol) prior to electrophoretic transfer that was carried out on ice, in transfer buffer at 100 V (constant voltage) for 145 minutes. The efficiency of

electrophoretic transfer was verified by staining immobilised proteins on PVDF membranes with Ponceau S solution (0.1 % Ponceau S, 5 % acetic acid; Sigma-Aldrich) by standard procedure.

Subsequently, PVDF membranes were incubated overnight at 4 °C in blocking buffer containing 5 % bovine serum albumin (BSA; Sigma-Aldrich), 0.05 % Triton 100 in PBS. Blocked membranes were incubated overnight at 4°C with primary antibodies diluted 1:1000 in blocking buffer. Membranes were then washed 5 times for 5 minutes each in washing buffer (0.05 % Triton 100 in PBS; PBS-T) and incubated for 45 minutes at room temperature with the corresponding horseradish peroxidase (HRP) conjugated secondary antibodies (1:1000 in PBS-T containing 5 % non-fat milk (Sigma-Aldrich)). Membranes were then washed 5 times for 5 minutes each in PBS-T and then incubated in ECL Western Blotting Substrate (Medical Supply) and further visualised on Fuji medical X-Ray films (Fujifilm Global) to detect signal.

Primary antibodies used for immunoblot analysis were paxillin (#610620; Becton, Dickinson and Company), GAPDH (#2118; Cell Signaling Technology), RAS (#OP40; Calbiochem), CDC42 (#sc-87; Santa Cruz Biotechnology). Secondary antibodies were horse anti-mouse IgG (heavy and light chain) HRP conjugated (#7076; Cell Signaling Technology) and goat anti-rabbit IgG (heavy and light chain) HRP conjugated (#7074; Cell Signaling Technology).

RESULTS

Effect of SK&F96365 on growth factors regulated cytoplasmic levels of Ca^{2+} and cell division - The selective inhibitor of store-operated Ca^{2+} influx, SK&F96365 [11,15] inhibits the proliferation of a variety of cell types [12–15] but its effect on human non-transformed MRC-5 fibroblast cells line has not been investigated to date. Thus, initial experiments were performed to establish the effect of SK&F96365 on cytoplasmic Ca^{2+} levels and proliferation in MRC5 cells. Measurement of Fura-2 fluorescence revealed a typical biphasic elevation of the cytoplasmic [Ca^{2+}] when quiescent MRC-5 fibroblasts were stimulated with FBS. An initial peak of cytoplasmic [Ca^{2+}] was followed by an elevated plateau (Fig 1A). However, when quiescent cells were stimulated with FBS in the presence of SK&F96365, although the initial peak of cytoplasmic [Ca^{2+}] was similar to that observed when cells were stimulated with FBS alone, the subsequent plateau of [Ca^{2+}] was much lower. These data are consistent with inhibition of Ca^{2+} influx by SK&F96365, which has been observed in several other cell lines.

Insert Figure 1 here

To investigate the effect of SK&F96365 on the proliferation of MRC-5 cells and progression through the cell cycle, cellular DNA content was measured by flow cytometry. Comparison analysis between quiescent cells and cell stimulated with FBS showed a statistically significant decrease in the percentage of cells in G_0/G_1 (from 91.0 % to 50.8 %) and a statistically significant increase in the percentage of the cells in S phase (from 1.7 % to 46.2 %). No difference in the percentage of cells in G_2/M between quiescent cells and cells stimulated with FBS was observed. Similar observations were made when comparing cells stimulated with FBS in the absence and presence of SK&F96365. A statistically significant

decrease in the percentage of cells in G_0/G_1 (from 83.6 % to 50.8 %) and a statistically significant increase of the percentage of cells in S phase (from 5.2 % to 46.2 %) was observed in cells stimulated with FBS alone when compared to the cells incubated with FBS in the presence of SK&F96365. As expected no difference in the percentage of cells in G_0/G_1, S and G_2/M was observed when comparing quiescent cells to cells stimulated with FBS in the presence of SK&F96365 (Fig 1B). The decreased percentage of cells in G_0/G_1 and increased percentage of cells in S phase 20 h after stimulation with FBS may suggest that cells have entered the cell cycle. A similar percentage of cells in G_0/G_1, S and G_2/M between quiescent cells and cells stimulated with FBS in the presence of SK&F96365 may suggest that SK&F96365 at the concentration of 60 µM inhibits FBS induced cell proliferation by arresting cells in G_0/G_1.

The effect of SK&F96365 was dose dependent, and the percentage of cells in G_0/G_1 rose gradually for concentrations ranging from 0 to 60 µM and subsequently persisted at a similar level for concentrations ranging 60 µM to 100 µM (Fig 1C). This suggests that at a concentration of 60 µM SK&F96365 reached its maximum effectiveness on MRC-5 cells and that further increasing the concentration of SK&F96365 had no effect on the percentage of cells in G_0/G_1. Based on these results 60 µM SK&F96365 was accepted as the most effective dose and used in subsequent experiments.

To support the observation that SK&F96365 inhibits cell division, an analysis of cell proliferation was performed. Comparison of the CFSE fluorescent intensity of quiescent cells stimulated with FBS cells arrested in G_0/G_1 showed a statistically significant decrease in the CFSE intensity between quiescent cells and cells stimulated with FBS 48 h after stimulation. The intensity of CFSE of cells stimulated with FBS was 44 % lower than the CFSE intensity of

quiescent cells. Similar observation was made when comparing the CFSE intensity of cells stimulated with FBS in the absence and presence of SK&F96365. A statistically significant decrease in CFSE fluorescent intensity (40 %) was observed in cells treated with FBS in the presence of SK&F96365 when compared to the cells incubated in FBS alone. No difference in the CFSE fluorescent intensity between quiescent cells and cells stimulated with FBS in the presence of SK&F96365 was observed (Fig 1D). The decreased CFSE intensity of cells stimulated with a mixture of FBS when compared to the CFSE intensity of quiescent cells may suggest that cells have gone through cell division. The similar CFSE intensity observed for quiescent cells and cells stimulated with FBS in the presence of SK&F96365 may suggest that SK&F96365 blocked the FBS induced proliferation of the cells.

Many pharmacological inhibitors show side effects and treatment of cells with chemical compounds can affect cell viability. Thus, to investigate if SK&F96365 at the concentration of 60 µM has a toxic effect on MRC-5 cells, the effect of SK&F96365 was evaluated by PI exclusion by live cells. Comparison analysis showed an increase from 1.7 % to 4.6 % in PI positive cells stimulated with growth factors in the presence of SK&F96365 when compared to cells stimulated with growth factors alone. A similar observation was made when comparing cells treated with FBS in the presence of SK&F96365 to the cells incubated with FBS alone. Treatment of cells with SK&F96365 increased the percentage of PI positive cells from 2.1 % to 4.5 %. An increased number of the PI positive cells in the presence of SK&F96365 may suggest that SK&F96365 has little toxic effect on MRC-5 cells (Supplementary Fig S-1). The observation of low toxic effects of SK&F96365 in the MRC-5 cell line was further supported by assessment of the reversibility of cell treatment with SK&F96365. Treatment of cells with inhibitor induced cell rounding and retraction and this

effect of SK&F96365 on cell morphology was reversible as removing of inhibitor from the culture medium caused reversible changes towards fibroblast, spindle-like morphology (Supplementary Fig S-2). In addition to changes in cell morphology, the process of fibroblast migration was completely abolished in the presence of SK&F96365. The functional activity of the cells was fully recovered after removal of inhibitor from culture medium (Supplementary Fig S-3).

Experimental strategy and workflow for global nLC-MS/MS analysis of Ca^{2+} regulated protein expression changes in G_1 phase - Our data has shown that SK&F96365 efficiently reduces serum growth factors regulated cytoplasmic level of Ca^{2+} and that this reduction in the level of cytoplasmic Ca^{2+} is associated with an inhibition of cell proliferation by arresting cells in G_0/G_1 phase. Thus, we next sought to investigate the extent to which inhibition of Ca^{2+} signalling may influence the profile of growth factor induced protein expression early in G_1 phase of the cell cycle by label-free nLC-MS/MS. For the nLC-MS/MS discovery experiment, MRC-5 cells were initially arrested in G_0/G_1 phase and then released from the arrest by stimulation with a defined mixture of growth factors containing EGF, dexamethasone, apo-transferrin, insulin and albumin from bovine serum to precisely control pathways that are activated upon re-stimulation to cell cycle entry. To investigate the effect of Ca^{2+} influx on protein expression changes, cells were stimulated in the absence and presence of SK&F96365. Treatment was stopped three hours after stimulation – this being the time close to the transition of cells from G_0 to G_1 phase. Sample preparation, acquisition and data analysis were carried out according to the workflow shown in Fig 2. In brief, samples for the nLC-MS/MS discovery experiment were lysed in SDS-based lysis buffer. Extracted proteins were then quantified using the BCA assay and equal amounts of

protein from each sample were digested with endoproteinase LysC and trypsin according to the FASP protocol [38]. To ensure that equivalent amounts of peptide material were loaded onto the Q-Exactive, peptides from the FASP digestion were quantified via NanoDrop. Next, peptides were desalted and purified on StageTips [39]. To achieve highly reliable results, the cell treatment and sample preparation for mass spectrometry analysis was performed on three independent days. Each biological sample was analysed as a technical replicate on the Q-Exactive in one combined run. The efficiency of cell treatment with the defined mixture of growth factors in the presence and absence of SK&F96365 was evaluated by flow cytometry each time the samples were prepared for mass spectrometry analysis. The quality of the raw data from the Q-Exactive analysis was visually inspected with Xcalibur™ software and then data were imputed into MaxQuant software for feature identification and detection [42]. Statistical analysis of the data and further selection of statistically important proteins was performed with Perseus software. The panel of proteins that were selected by statistical analysis were next subjected to pathway analysis (IPA software) to map these proteins to pathways and biological processes in which selected proteins could play a role. The expression of three proteins selected by statistical analysis and found to be involved in cell cycle regulation was validated by Western blot analysis to corroborate findings from analysis of the nLC-MS/MS data.

Insert Figure 2 here

Proteomic analysis of Ca^{2+} regulated protein expression changes in G_1 phase - In order to investigate the observed global protein expression changes in response to the inhibition of Ca^{2+} influx, label-free nLC-MS/MS analysis was performed. Effective interpretation of the comprehensive nLC-MS/MS proteomic data for the purpose of mechanistic insight requires

a robust and reproducible strategy to acquire this data. Thus, the first step in nLC-MS/MS data analysis was to establish the extent to which processes applied during this study were reproducible in order to further decide on the statistical threshold to be applied. Visual inspection of the raw MS data showed normal distribution of total ion chromatograms (TICs) and highly consistent TIC's between technical (Fig 3A) and biological (Fig 3B) replicates. Moreover, comparison of the intensities (LFQ) of individual proteins revealed an average Pearson correlation of 0.99 for both technical (Fig 3C) and biological (Fig 3D) replicates, thus confirming good quantitative correlation of the data. Database searching of the MS/MS data (see Experimental Procedures) resulted in the identification of around 4,000 proteins in each individual cell lysate. Both technical replicates (n=2) and biological replicates (n=3) showed an average of 95 % overlap in proteins identified (see Fig 3E and Fig 3F). Detailed data showing the reproducibility between technical and biological replicates including qualitative analysis, TICs, correlation plots and overlap in protein identification can be found in Supplementary FigsS-4, S-5 and S-6. This data demonstrates that highly reproducible and comprehensive analysis of protein expression was obtained from analysis of total cell lysates of non-transformed primary human lung fibroblasts (MRC-5 cells). In these and subsequent experiments a total of 4,411 proteins were identified from MRC-5 cells across all conditions with high confidence (false discovery rate < 1 %; for details see Supplementary Table 1).

Insert Figure 3 here

To identify proteins that are regulated by the inhibition of Ca^{2+} influx, statistical analysis of the 4,411 identified proteins was performed. Of over 4,000 proteins measured, incubation of cells with growth factors in the presence of SK&F96365 (60 µm) had a significant effect on the expression of 182 proteins (Fig 4A and Table 1). Of the proteins changing in the presence

of SK&F96365, 71 were significantly up-regulated and 111 were significantly down-regulated (see Supplementary Table 2).

Insert Table 1 here

Furthermore, the comparison of protein expression levels for all proteins measured in cells treated with purified growth factors in the absence and presence of SK&F96365 showed a very strong overall negative correlation (Supplementary Fig S-7). This shows that, for the most part, changes in protein expression under both conditions follows an opposing trend in expression - proteins that are up-regulated with growth factors were down-regulated in cells incubated with growth factors in the presence of SK&F96365. Similarly, most of the proteins that were down-regulated in cells treated with growth factors were up-regulated in cells with inhibited Ca^{2+} influx.

Insert Figure 4 here

In order to identify proteins that may play a crucial role in Ca^{2+} dependent regulation of growth factor induced proteins in the G_1 phase of the cell cycle, grouping of statistically significant proteins into hierarchical clusters and principle components was performed. Unsupervised hierarchical clustering of 291 proteins that were found to be differentially expressed between the four conditions used in these experiments resulted in clear grouping of the biological replicates and a clear distinction between the different conditions (Fig 4B). Fig 4B shows that the protein expression pattern of cells incubated with growth factors and treated with SK&F96365 (G+) were most closely related to the expression pattern observed in control (quiescent) cells (C). More importantly, some of the proteins whose expression is regulated by SK&F96365 are likely to play a role in growth factor induced G_1 and cell cycle

progression. When analysing the expression profile of proteins between all four conditions, the most interesting were clusters where the protein expression profile was similar for the following conditions; control (quiescent) cells (C), control (quiescent) cells treated with SK&F96365 (C+) and cells incubated with growth factors and treated with SK&F96365 (G+) but the expression of these proteins was opposite in the cells incubated with growth factors (G). These clusters represent proteins that were not affected by the treatment of quiescent cells with SK&F96365, the growth factor stimulation has altered the expression of these proteins but the effect of growth factor stimulation was attenuated when cells were treated with SK&F96365. Proteins identified in these clusters are summarised in Table 2.

Insert Table 2 here

Fig 4C shows principal component analysis of the data and reveals that the first component separates samples based on the treatment of cells with growth factors and component 2 separated samples according to treatment with SK&F96365. Both principal components represent panels of proteins and it was on the expression levels of these proteins that the separation between conditions was based. Of interest are the proteins that separate samples based on treatment with SK&F96365 and these include; ARHGEF17, ASPSCR1, BAK1, BNIP3L, CASP7, CDC26, CDH2, CIT, CRYL1, CTGF, ERC2, EXOSC8, GTF2H4, GTF3C1, HIGD1A, HMG20A, MCM3, METTL3, MRPL22, NR4A1, PBRM1, PTAR1, QPCTL, RCL1, SLC30A9, TJAP1 and TMOD2 (for more details see Table 3).

Insert Table 3 here

In this part of analysis we have identified proteins that appear to be regulated by the inhibition of Ca^{2+} influx. Additionally, hierarchical clustering and principle component

analysis allowed to prioritise proteins that are more likely to be involved in Ca^{2+} dependent regulation of the cell cycle.

Biological interpretation of the data - Biological interpretation of big data sets from proteomic screens is a very challenging task. The biggest difficulty is the extraction of functional and biological knowledge from the long list of proteins generated during mass spectrometry discovery experiments. In recent years pathway analysis has become the first choice for understanding and interpretation of the biological significance of the datasets of proteins expressed under specific conditions which are generated during proteomic discovery experiments [45–48]. Thus, to interpret the biological significance of proteins differentially expressed by the inhibition of CCE (panel of 182 proteins), an analysis of canonical pathways and biological processes was performed using Ingenuity Pathway Analysis (IPA) software.

An initial pathway analysis was performed to determine canonical pathways that were regulated by the inhibition of Ca^{2+} influx. The top 15 canonical pathways selected by IPA were: PI3K/AKT signalling, FAK signalling, mTOR signalling, 14-3-3-mediated signalling, insulin receptor signalling, integrin signalling, IGF-1 signalling, regulation of cellular mechanics by calpain protease, EGF signalling, protein ubiquitination pathway, ErbB signalling, PAK signalling, epithelial adherens junction signalling, actin nucleation by ARP-WASP complex. Importantly, these pathways can be grouped to the pathways that regulate cell proliferation for example PI3K/AKT signalling, insulin receptor signalling, EGF signalling, ErbB signalling and pathways that regulate the morphology of the cells for example FAK signalling, integrin signalling, PAK signalling, epithelial adherens junction signalling or actin nucleation by ARP-WASP complex (data not shown).

Subsequently ontology enrichment analysis of the 182 proteins whose expression was altered by treatment with SK&F96365 was then performed to determine which of the cellular processes were affected by Ca^{2+} influx inhibition. A total of 182 proteins differently expressed in the cells with inhibited Ca^{2+} influx were grouped into following categories: cellular growth and proliferation, cell cycle, cell morphology, cellular assembly and organisation, cellular movement, DNA replication, recombination and repair, molecular transport, protein degradation, protein synthesis, RNA post-transcriptional modification, cell death and survival, and cell to cell signalling and interaction. A summary of the ontology enrichment analysis associated with this dataset can be found in Table 4.

Insert Table 4 here

It is well established that growth factors acting alone cannot stimulate cell division and cells must receive appropriate environmental cues from cell-substrate adhesion [49,50], cell shape [51–53] and cell-cell contact [54] to progress through the G_1 phase of cell cycle up to the R point. Our data suggests that Ca^{2+} could be a factor that links cell proliferation with the environmental cues, cells morphology and cellular assembly and organisation by the regulation of the expression of proteins that play a role in all three processes. Subsequently, to determine common proteins involved in the regulation of these processes an overlap analysis was performed. Forty of the 182 proteins identified as proteins regulated by Ca^{2+} inhibition were found to be associated with cell proliferation, morphology and cellular assembly and organisation. Ten proteins have been identified as common proteins involved in the regulation of all selected for analysis categories. These proteins included ACP1, CDC42, EGFR, F2R, ERBB4, HRAS, IKBKB, PIK3R1, PAX and RHOB. Some proteins such as AKT3, EEF1D, EIF3I, EPB41L3, PBXIP1, TSC2, TSG101, TSNAX, TXNIP and UBE2D3 have been

exclusively associated with cell proliferation. ABCD1, ARHGEF17, ATG4B, BCS1L, EPB41, RHOJ and TBCD were exclusive to the process of cellular assembly and organization and RAP2B and TSC2 were found to regulate cell morphology. Ten proteins, VPS4A, CDC42BPA, ARFGEF1, CTNNA2, NCKAP1, MAP1B, UCHL1, TBCE, KIF3B and IOP9 were identified as proteins involved in the regulation of cell morphology and cellular assembly and organization. CDK4 was common in cell proliferation and assembly and organisation. None of the proteins were common for cell proliferation and morphology (Fig 5).

Insert Figure 5 here

The IPA analysis of biological importance of the data has indicated that Ca^{2+} signalling may regulate cell proliferation via PI3K/AKT signalling and its downstream target mTOR. In addition, some other canonical pathways identified such as FAK, integrin, PAK, epithelial adherents junction were found to be regulated by Ca^{2+} influx inhibition and associated with the regulation of cell morphology and cellular assembly and organisation.

Validation of protein expression changes - Proteomic discovery experiments are very complex experiments in terms of sample preparation, acquisition and data analysis. Each of the steps that are undertaken in proteomic workflow may then account for the variables and errors in the estimation of proteins that are differently expressed between investigated conditions, termed false discovery rate. Thus, it is important to verify the findings by alternative methods applied to investigate protein expression changes for example Western blotting [55], Elisa [56] (applied mostly for the secreted proteins), multiple reaction monitoring (MRM) [57–59] or imaging followed by staining with specific antibodies [60]. Accordingly, to confirm whether the protein expression changes observed in nLC-MS/MS analysis are authentic findings, an analysis of protein expression levels of three selected

proteins was performed using Western blotting. These proteins, paxillin, HRAS and CDC42 (proteins marked with asterisks on Fig 5), were selected based on their involvement in cellular processes relevant to cell cycle progression and the regulation of cell morphology and cellular assembly and organisation. The nLC-MS/MS data obtained for all three proteins indicated that they were down-regulated (moderately but with statistical significance) in the presence of SK&F96365. Western blot analysis of paxillin (Fig 6A-B), RAS (Fig 6C-D) and CDC42 (Fig 6E-F) showed they were all expressed at lower average levels in cells treated with SK&F96365. Further density analysis of these proteins bands has shown that the relative change of the bands normalised to the density of the internal control GAPDH was lower in cells treated with growth factors in the presence of SK&F96365 when compared to cells incubated in the presence of growth factors alone. However, only for paxilin this change was statistically significant. This data is in close agreement with the nLC-MS/MS analysis and provides good evidence to support the authenticity of the nLC-MS/MS dataset of Ca^{2+} influx dependent changes in protein expression (see Supplementary Table 2). To date this independent validation of individual protein expression changes has been undertaken on 3 proteins. Additional data from Western blot validation are in Supplementary Fig S-8.

Insert Figure 6 here

DISCUSSION

To our knowledge, this is the first study to report the effect of Ca^{2+} signalling on growth factor induced protein expression in human non-transformed cells on a proteomic scale. Ca^{2+} is universally required for cell cycle progression in non-excitable cells, including fibroblasts [6]. Here we show that SK&F96365, an inhibitor of store-operated Ca^{2+} entry, decreases the plateau of serum growth factor induced Ca^{2+} levels without affecting the initial transient increase in Ca^{2+} in human fibroblasts as previously reported for other cell types [9,16,61]. This reduced level of sustained cytoplasmic Ca^{2+} inhibits cell progression to S phase [9,16] an observation shown here for human fibroblasts. Although the role of Ca^{2+} in the cell cycle is well established and, as noted above, several studies have shown that the inhibition of Ca^{2+} influx by pharmacological agents blocks the proliferation of fibroblasts [12], epithelial cells [7], brain tumor cells [13] and peripheral blood lymphocytes [14], the molecular mechanism(s) by which Ca^{2+} signalling regulates these events in G_1 phase is poorly characterised. In particular, the requirement for and impact of Ca^{2+} influx on growth factor induced gene expression during the early stages of G_1 has received little attention. To address this, we have analysed, on a global proteomic scale, the effect of inhibition of Ca^{2+} influx on growth factor induced protein expression changes early in G_1. Using high-resolution mass spectrometry together with the rigorous sample preparation we have routinely identified just over 4,000 proteins in each experimental sample. Whilst the mass spectrometry data reported is highly robust and reproducible there are of course significant limitations associated with the use of small molecule inhibitors as employed here. Inhibitors, such as SK&F96365, may be expected to exhibit low specificity and off-target effects. To partially address this issue and to evalaute the effectiveness of an inhibitor it is

common to investigate and report the concentration of the molecule which is required to induce a half-maximal inhibitory effect (IC_{50}). In many of the experiments described here the optimal inhibitory concentration of SK&F96356 was 60 µM and an IC_{50} of ~30 µM was observed. Both are close to the upper limits reported by others [14,15] and suggest that, in the experiments reported here SK&F96365 may have off target (non-specific) effects. Notably, in addition to its effect on various Ca^{2+} channels at high concentrations SK&F96365 may also inhibit K^+ currenst [62]. Notably, Labelle *et al*. [63] have shown that SK&F96365 may inhibit cytochrome P450 and prostaglandin E_2 pathways but that this does not account for the ability of the drug to inhibit cell proliferation. It is evident therefore that the potential direct association of Ca^{2+} influx and the protein changes reported here will require further investigation.

The global analysis presented in this manuscript represents the data of single time point analysis of two highly dynamic and time dependent processes of cell division and Ca^{2+} influx. Indeed, addition of another time point or using different cell treatment pattern (for example treatment of cells with SK&F96365 30 minutes after addition of growth factors) would improve confidence of current findings. Nevertheless, even in light of these limitations, the data presented here provide a valid source of information of complete set of protein expression changes regulated by Ca^{2+}, their rates of change and involvement in the regulation of biological processes. Furthermore, identified proteins provide numerous opportunities for more detailed investigations of the mechanism of Ca^{2+} dependent regulation of cell cycle at the molecular and systemic level.

Evaluation of data quality by analysis of features such as; distribution of total ion current chromatograph (TIC) traces, proteome coverage and protein LFQ intensities between

technical and biological replicates has shown that applied in this project nLC-MS/MS strategy is robust and reproducible. Normal distribution of TIC's traces and highly consistent total ion current chromatograms between technical and biological replicates (Fig 3A-B) has confirmed that unlikely any variances have been introduced at the level of sample preparation or sample acquisition. High similarity in LFQ intensities of measured proteins between technical and biological replicates with Pearson correlation 0.99 assured good reproducibility in measured proteins intensities. In addition, most of the proteins have been identified in each technical and biological replicates and only 5 % of the total number of proteins identified was represented by missing values. Notably, good correlation has been found across the output data from different analysis steps. For example, hierarchical clustering and PCA analysis grouped the samples according to the replicates and each treatment condition was clearly separated. In addition, IPA analysis indicated that processes of fibroblast proliferation, cell shape changes and cell migration may be negatively regulated in cells treated with SK&F96365. Subsequent functional analysis of these biological processes have confirmed that cells treated with SK&F96365 (i) do not proliferate and are arrested in G_0/G_1 (Fig 1B-D), (ii) have altered morphology (Supplementary Fig S-2) and (iii) do not migrate (Supplementary Fig S-3). Altogether, this data demonstrates that highly reproducible and comprehensive analysis of protein expression was obtained using total cell lysates of non-transformed primary human lung fibroblasts (MRC-5 cells).

Statistical analysis of 4411 common proteins identified between all experimental conditions has shown that incubation of cells with growth factors in the presence of SK&F96365 (60 μM) significantly changed the expression of 182 proteins (Fig 4A). To the protein expression changes observed in this study several mechanisms can contribute for example activation of

immediate early genes [64] and further transcription and translation of the protein [65]. Some other processes such as protein stabilisation (associated with increased protein abundance) or protein degradation (accompanied by the decrease in protein abundance) [66] also contribute to these protein expression changes. Data presented in here has shown that majority of the proteins (111 proteins) were found to be down-regulated in presence of SK&F96365 and this in turn may suggest that Ca^{2+} at selected time point more likely regulates the mechanism(s) associated with stabilisation, transcription and translation of the protein. Further application of hierarchical clustering and PCA analysis has shortlisted a number of proteins regulated significantly by Ca^{2+} influx. Selected by this analysis proteins may provide possible insights into Ca^{2+} dependent regulation of G_1. For example, one possibility is that Ca^{2+}, by affecting protein expression, may disrupt the interaction between the RHOA protein [67] and its activator Rho guanine nucleotide exchange factor 17 (ARHGEF17). Importantly, GSN, TUBB and CTNNA2 proteins, which were also found to change here, have previously been shown to interact with ARHGEF17 [68] (for details see Supplementary Table 2). In contrast to ARHGEF17, which was upregulated, the interacting proteins were down regulated. Some other proteins identified here including TMOD2 (or CIT) have also been shown to be connected with ARHGEF17 and RHOA [69,70]. Importantly, it appears that all these proteins create a network associated with the regulation of the cytoskeleton and cell proliferation with RHOA being the central node. Elegant studies conducted by Huang *et al.* [71] have demonstrated a possible link between proteins that are involved in the regulation of cell shape and cell cycle progression. Changes in cell morphology, such as cell rounding (a process that was also observed in this study; Supplementary Fig S-2) and cytoskeletal reorganisation are associated with decreased levels of cyclin D and an increased level of CKI, the $p27^{Kip1}$. These two key proteins are involved in

the transition of cells through the R point, late in G_1 phase. Interestingly, Hu *et al.* have shown that the degradation of $p27^{Kip1}$ depends on RHOA [72] and it is possible that Ca^{2+} signalling may be necessary for the RHOA dependent degradation of $p27^{Kip1}$. The above evidence supports a possible mechanism in which the altered expression of ARHGEF17 and its interacting partners limit the activation of RHOA and subsequent degradation of $p27^{Kip}$. Under these conditions the cyclin E/CDK2 complex would remain inactive so arresting cells in G_1 at the R point (for details see Fig 7). The observation that Ca^{2+} plays a role at the R point transition has been reported before [15,73]. Notably, it has been shown that Ca^{2+} regulates the expression of two key G_1 phase regulatory proteins, cyclin D [74] and cyclin E [15] at the restriction point. In addition, it has been shown that Ca^{2+} is involved in the regulation of expression of $p21^{Cip1/Waf1/Sdi1}$ and $p27^{Kip1}$ with inhibition of Ca^{2+} influx resulting in up-regulation of both $p21^{Cip1/Waf1/Sdi1}$ [19,75] and $p27^{Kip1}$ [15] and cell cycle arrest at R [30].

Insert Figure 7 here

Some interesting observations and conclusions came also from the IPA analysis of 182 proteins which expression was found to be regulated by Ca^{2+} influx inhibition. Interestingly, this analysis has indicated that the inhibition of Ca^{2+} influx in MRC-5 cells likely affects the proliferation of the cells via the regulation of canonical PI3K/AKT signalling and its downstream target mTOR. A study by Gao *et al.* has shown that the inhibition of PI3K/AKT by LY294002 inhibitor in prostate cancer cell lines DU145 and PC-3 decreases the phosphorylation of AKT and the expression of the key cell cycle molecules such as cyclin D1, CDK4 [76]. In addition, treatment of cells with LY294002 upregulates the expression of cyclin kinase inhibitor $p21^{CIP1/WAF1}$ and prevents the phosphorylation of Rb protein at Ser780, Ser795 and Ser807/811 [76]. Casagrande *et al*. have reported similar observation in the

choroidal melanoma cell, demonstrating that the treatment of cells with the LY294002 inhibitor upregulates the expression of cyclin kinase inhibitor $p27^{Kip1}$ and prevents functional activity of CDK4 and CDK2[77]. Furthermore, Gao *et al.* have shown that inhibition of PI3K/AKT by LY294002 affects the function of AKT downstream target, the mammalian target of rapamycin (mTOR) and prevents the phosphorylation of mTOR substrate the $p70^{S6K}$ protein involved in the regulation of the expression of $p21^{CIP1/WAF1}$ and G_1/S transition[76]. Blocking the mTOR pathway with inhibitors such as rapamycin or PI-103 prevents cell proliferation by cell cycle arrest in G_0/G_1 phase. The subsequent molecular mechanism involves downregulation of cyclin D1 and E1 and upregulation of $p21^{CIP1/WAF1}$, $p27^{Kip1}$ and p53 [78,79]. Thus, it is possible that proteins selected by IPA analysis such as MAPKAP1, RHOB, PIK3R1, TSC2, EIF3I, AKT3, HRAS, RHOJ or IKBKB contribute to the described Ca^{2+} dependent mechanisms of PI3K/AKT and mTOR regulation of cell cycle.

When quiescent cells (in G_0) are exposed to growth factors and mitogens a series of intracellular signalling events are initiated that control entry into and progression through G_1. However, growth factors acting alone cannot stimulate cell division and the presence of appropriate environmental stimuli from cell-substrate adhesion [49,50], cell shape [51–53] and cell-cell contact [54] cells must be provided for successful progression through the G_1 phase of cell cycle up to the R point. Notably, in addition to cell proliferation some pathways identified by IPA such as FAK, integrin, PAK, epithelial adherents junction signalling and actin nucleation by ARP-WASP complex are associated with the regulation of the cell-substrate adhesion, cell shape and cell-cell contact. Accordingly, the analysis of biological processes has indicated that indeed cellular assembly and organisation and cell morphology are the processes regulated by the inhibition of Ca^{2+} influx. In addition, IPA analysis predicted that

processes such as cell shape, cell spreading and most of the processes associated with the cellular assembly and organisation (Table 4) may be negatively regulated in cells treated with SK&F96365. Interestingly, comparative analysis of cell proliferation, cell morphology and cellular assembly and organisation has indicated proteins that are involved in all three processes. The common proteins identified ACP1, CDC42, EGFR, IKBKB, ERBB4, F2R, RHOB, HRAS, PIK3R1 and PAX may be potential candidates that could link Ca^{2+} signalling with the cell shape and/or cell substrate adhesion dependent regulation of G_1 phase. One attractive scenario could be that Ca^{2+} signalling regulates the expression or activity of proteins that belong to the family of small GTPases that are known to regulate cell shape, cellular assembly and organisation and proliferation. Indeed three proteins HRAS, CDC42 and RHOB that belong to the family of small GTPases have been identified in the panel of common proteins. Expression of all of these proteins was found to be down-regulated in the presence of SK&F96365. Subsequent analysis of the importance of these proteins by scientific groups has established their role in cell cycle progression. Unquestionably, RAS, RHO and CDC42 proteins are necessary for cell cycle progression, most importantly progression through the G_1 phase of cell cycle [80]. It is also evident that all of these proteins play a role in cell adhesion and morphology. For example, it has been reported that overexpression of a dominant negative mutant of CDC42 inhibits integrin-dependent cell spreading [81]. At the same time microinjection of constitutively activated CDC42 to quiescent Swiss 3T3 fibroblasts induces G_1 progression and DNA synthesis [82]. The importance of H-RAS has been demonstrated by the observation that the downregulation of its expression by siRNA reduces proliferation of T80H cells (by cell cycle arrest in G_0/G_1 phase) [83] and the overexpression of H-RAS in normal human fibroblasts alters cell shape causing rounding up of the cells [84]. Notably, the activation of RAS occurs immediately and transiently following

addition of growth factors to quiescent cells and then again in mid G_1 [85] and both the RAS-Raf-Mek-Erk and RAS-PI3K-PDK1-AKT/PBK signalling pathways are required for cell cycle entry and progression through G_1 [86–88]. As shown by multiple studies, the main function of RAS protein in G_1 phase progression is to inactivate Rb protein, the key molecular mechanism that drives the transition of the cells from G_1 to S phase [89,90]. RHOB seems to have a negative effect on cell proliferation through its ability to supress the K-RAS, N-RAS or H-RAS oncogenes [91]. However, in prostate cancer cell lines down-regulation of RHOB reduces cell spreading, alters cell morphology [92] but has no effect on cell proliferation [93]. Ca^{2+} influx dependent changes were also observed in the expression of paxillin. The important role of this protein in cell cycle progression has been well documented and numerous studies have shown that overexpression of paxillin mRNA and stabilisation of protein by phosphorylation increase the rate of cell proliferation [94,95]. As might be expected, siRNA mediated down-regulation of paxillin expression significantly inhibits cell cycle progression [95].

Conclusions: In summary, the results presented here demonstrate the application of mass spectrometry based proteomics in the analysis of Ca^{2+} dependent regulation of cell cycle. Careful experimental design, the application of robust sample preparation methods, and the use of sensitive mass spectrometry resulted in highly reproducible and comprehensive analysis of protein expression changes in non-transformed primary human lung fibroblasts (MRC-5 cells). Application of this highly robust and accurate proteomic workflow allowed the identification of 182 novel proteins regulated by Ca^{2+} signalling. The data presented in here represents the biggest to date dataset of proteins regulated by Ca^{2+} signalling and provides numerous opportunities for more detailed investigations of the mechanism of Ca^{2+}

dependent regulation of cell cycle at the molecular and system level. Proposed in here possible mechanism is one attractive scenario, which can be used as a starting point to begin this type of the research. Moreover, the data highlights that identified proteins in addition to the regulation of cell division are also involved in the regulation cell morphology and cellular assembly and organization, the environmental clues, which are known to regulate cell proliferation. Common proteins involved in the regulation of these processes may provide the link between Ca^{2+}, cell morphology and cell proliferation an environmental cues on which division depends.

The comprehensive proteomic dataset reported here has been made publically available (http://proteomecentral.proteomexchange.org) and provides a rich source of information that will underpin further investigation of the molecular mechanism(s) of Ca^{2+} influx dependent regulation of mammalian cell cycle entry and cell cycle progression to G_1 and beyond. We suggest that this may pave the way for a more detailed and comprehensive temporal survey of Ca^{2+} dependent regulation of growth factor induced protein expression changes as cells progress through the cell cycle.

All mass spectrometry proteomics data have been uploaded to the ProteomeXchange Consortium (http://proteomecentral.proteomexchange.org) via the PRIDE. Dataset can be accessed using identifier PXD002303.

REFERENCES

[1] Bruce A, Alexander J, Julian L, David M, Martin R, Keith R, et al. Molecular Biology of the Cell, 6th Ed. Garland Science; 2014.

[2] Rhind N, Russell P. Signaling pathways that regulate cell division. Cold Spring Harb Perspect Biol 2012;4:a005942.

[3] Hanahan D, Weinberg RA. Hallmarks of cancer: the next generation. Cell 2011;144:646–74.

[4] Kastan MB, Bartek J. Cell-cycle checkpoints and cancer. Nature 2004;432:316–23.

[5] Lapenna S, Giordano A. Cell cycle kinases as therapeutic targets for cancer. Nat Rev Drug Discov 2009;8:547–66.

[6] Barbiero G, Munaron L, Antoniotti S, Baccino FM, Bonelli G, Lovisolo D. Role of mitogen-induced calcium influx in the control of the cell cycle in Balb-c 3T3 fibroblasts. Cell Calcium 1995;18:542–56.

[7] Ichikawa J, Kiyohara T. Suppression of EGF-induced cell proliferation by the blockade of Ca2+ mobilization and capacitative Ca2+ entry in mouse mammary epithelial cells. Cell Biochem Funct 2001;19:213–9.

[8] Takuwa N, Zhou W, Kumada M, Takuwa Y. Involvement of Intact Inositol-1,4,5-Trisphosphate-Sensitive Ca2+ Stores in Cell-Cycle Progression at the G1/S Boundary in Serum-Stimulated Human Fibroblasts. Febs Lett 1995;360:173–6.

[9] Wahl M, Gruenstein E. Intracellular free Ca2+ in the cell cycle in human fibroblasts: transitions between G1 and G0 and progression into S phase. Mol Biol Cell

1993;4:293–302.

[10] Putney JW. A model for receptor-regulated calcium entry. Cell Calcium 1986;7:1–12.

[11] Merritt JE, Armstrong WP, Benham CD, Hallam TJ, Jacob R, Jaxa-Chamiec A, et al. SK&F 96365, a novel inhibitor of receptor-mediated calcium entry. Biochem J 1990;271:515–22.

[12] Jenkins RE, Hawley SR, Promwikorn W, Brown J, Hamlett J, Pennington SR. Regulation of growth factor induced gene expression by calcium signalling: integrated mRNA and protein expression analysis. Proteomics 2001;1:1092–104.

[13] Lee YS, Sayeed MM, Wurster RD. Inhibition of human brain tumor cell growth by a receptor-operated Ca2+ channel blocker. Cancer Lett 1993;72:77–81.

[14] Chung SC, McDonald T V, Gardner P. Inhibition by SK&F 96365 of Ca2+ current, IL-2 production and activation in T lymphocytes. Br J Pharmacol 1994;113:861–8.

[15] Chen Y-W, Chen Y-F, Chen Y-T, Chiu W-T, Shen M-R. The STIM1-Orai1 pathway of store-operated Ca(2+) entry controls the checkpoint in cell cycle G1/S transition. Sci Rep 2016;6:22142.

[16] Pennington SR, Foster BJ, Hawley SR, Jenkins RE, Zolle O, White MRH, et al. Cell shape-dependent control of Ca2+ influx and cell cycle progression in Swiss 3T3 fibroblasts. J Biol Chem 2007;282:32112–20.

[17] Liou J, Kim ML, Heo W Do, Jones JT, Myers JW, Ferrell JE, et al. STIM is a Ca2+ sensor essential for Ca2+-store-depletion-triggered Ca2+ influx. Curr Biol 2005;15:1235–41.

[18] Vig M, Peinelt C, Beck A, Koomoa DL, Rabah D, Koblan-Huberson M, et al. CRACM1 is

a plasma membrane protein essential for store-operated Ca2+ entry. Science 2006;312:1220–3.

[19] Faouzi M, Hague F, Potier M, Ahidouch A, Sevestre H, Ouadid-Ahidouch H. Down-regulation of Orai3 arrests cell-cycle progression and induces apoptosis in breast cancer cells but not in normal breast epithelial cells. J Cell Physiol 2011;226:542–51.

[20] Azimi I, Roberts-Thomson SJ, Monteith GR. Calcium influx pathways in breast cancer: Opportunities for pharmacological intervention. Br J Pharmacol 2014;171:945–60.

[21] Stewart TA, Yapa KTDS, Monteith GR. Altered calcium signaling in cancer cells. Biochim Biophys Acta 2015;1848:2502–11.

[22] Capiod T. Cell proliferation, calcium influx and calcium channels. Biochimie 2011;93:2075–9.

[23] Munaron L, Antoniotti S, Fiorio Pla A, Lovisolo D. Blocking Ca2+entry: a way to control cell proliferation. Curr Med Chem 2004;11:1533–43.

[24] Santella L, Ercolano E, Nusco GA. The cell cycle: a new entry in the field of Ca 2+ signaling. Cell Mol Life Sci 2005;62:2405–13.

[25] Katoch SS, Su X, Moreland RS. Ca2+- and protein kinase C-dependent stimulation of mitogen-activated protein kinase in detergent-skinned vascular smooth muscle. J Cell Physiol 1999;179:208–17.

[26] Choi YJ, Anders L. Signaling through cyclin D-dependent kinases. Oncogene 2014;33:1890–903.

[27] Sée V, Rajala NKM, Spiller DG, White MRH. Calcium-dependent regulation of the cell

cycle via a novel MAPK-NF-κB pathway in Swiss 3T3 cells. J Cell Biol 2004;166:661–72.

[28] Takuwa N, Zhou W, Kumada M, Takuwa Y. Ca(2+)-dependent stimulation of retinoblastoma gene product phosphorylation and p34cdc2 kinase activation in serum-stimulated human fibroblasts. J Biol Chem 1993;268:138–45.

[29] Cook SJ, Lockyer PJ. Recent advances in Ca(2+)-dependent Ras regulation and cell proliferation. Cell Calcium 2006;39:101–12.

[30] Roderick HL, Cook SJ. Ca2+ signalling checkpoints in cancer: remodelling Ca2+ for cancer cell proliferation and survival. Nat Rev Cancer 2008;8:361–75.

[31] Machaca K. Ca2+ signaling, genes and the cell cycle. Cell Calcium 2011;49:323–30.

[32] Pinto MCX, Kihara AH, Goulart VAM, Tonelli FMP, Gomes KN, Ulrich H, et al. Calcium signaling and cell proliferation. Cell Signal 2015;27:2139–49.

[33] Déliot N, Constantin B. Plasma membrane calcium channels in cancer: Alterations and consequences for cell proliferation and migration. Biochim Biophys Acta 2015;1848:2512–22.

[34] Ryan PA, Maher VM, McCormick JJ. Modification of MCDB 110 medium to support prolonged growth and consistent high cloning efficiency of diploid human fibroblasts. Exp Cell Res 1987;172:318–28.

[35] Wistrom C, Villeponteau B. Long-term growth of diploid human fibroblasts in low serum media. Exp Gerontol 1990;25:97–105.

[36] Bootman MD, Rietdorf K, Collins T, Walker S, Sanderson M. Ca2+-sensitive fluorescent dyes and intracellular Ca2+ imaging. Cold Spring Harb Protoc 2013;8:83–99.

[37] Kopach O, Vats J, Netsyk O, Voitenko N, Irving A, Fedirko N. Cannabinoid receptors in submandibular acinar cells: functional coupling between saliva fluid and electrolytes secretion and Ca2+ signalling. J Cell Sci 2012;125:1884–95.

[38] Wisniewski JR, Zougman A, Nagaraj N, Mann M. Universal sample preparation method for proteome analysis. Nat Meth 2009;6:359–62.

[39] Rappsilber J, Mann M, Ishihama Y. Protocol for micro-purification, enrichment, pre-fractionation and storage of peptides for proteomics using StageTips. Nat Protoc 2007;2:1896–906.

[40] Rappsilber J, Ishihama Y, Mann M. Stop And Go Extraction tips for matrix-assisted laser desorption/ionization, nanoelectrospray, and LC/MS sample pretreatment in proteomics. Anal Chem 2003;75:663–70.

[41] Turriziani B, Garcia-Munoz A, Pilkington R, Raso C, Kolch W, von Kriegsheim A. On-beads digestion in conjunction with data-dependent mass spectrometry: a shortcut to quantitative and dynamic interaction proteomics. Biology (Basel) 2014;3:320–32.

[42] Cox J, Mann M. MaxQuant enables high peptide identification rates, individualized p.p.b.-range mass accuracies and proteome-wide protein quantification. Nat Biotechnol 2008;26:1367–72.

[43] Cox J, Hein MY, Luber C a, Paron I. Accurate proteome-wide label-free quantification by delayed normalization and maximal peptide ratio extraction, termed MaxLFQ. Mol Cell Proteomics 2014;13:2513–26.

[44] Cox J, Neuhauser N, Michalski A, Scheltema RA, Olsen J V, Mann M. Andromeda: A

Peptide Search Engine Integrated into the MaxQuant Environment. J Proteome Res 2011;10:1794–805.

[45] Barabási A-L, Gulbahce N, Loscalzo J. Network medicine: a network-based approach to human disease. Nat Rev Genet 2011;12:56–68.

[46] Altelaar AFM, Munoz J, Heck AJR. Next-generation proteomics: towards an integrative view of proteome dynamics. Nat Rev Genet 2012;14:35–48.

[47] Wu X, Hasan M Al, Chen JY. Pathway and network analysis in proteomics. J Theor Biol 2014;362:44–52.

[48] Pieroni E, De La Fuente Van Bentem S, Mancosu G, Capobianco E, Hirt H, De La Fuente A. Protein networking: Insights into global functional organization of proteomes. Proteomics 2008;8:799–816.

[49] Otsuka H, Moskowitz M. Arrest of 3T3 cells in G1 phase in suspension culture. J Cell Physiol 1975;87:213–9.

[50] STOKER MGP. Growth inhibition of polyoma-transformed cells by contact with static normal fibroblasts. J Cell Sci 1966;1:297–310.

[51] Folkman J, Moscona a. Role of cell shape in growth control. Nature 1978;273:345–9.

[52] Ireland GW, Dopping-Hepenstal P, Jordan P, O'Neill C. Effect of patterned surfaces of adhesive islands on the shape, cytoskeleton, adhesion and behaviour of Swiss mouse 3T3 fibroblasts. J Cell Sci Suppl 1987;8:19–33.

[53] O'Neill C, Jordan P, Ireland G. Evidence for two distinct mechanisms of anchorage stimulation in freshly explanted and 3T3 Swiss mouse fibroblasts. Cell 1986;44:489–

96.

[54] Levine EM, Becker Y, Boone CW, Eagle H. Contact Inhibition, Macromolecular Synthesis, and Polyribosomes in Cultured Human Diploid Fibroblasts. Proc Natl Acad Sci U S A 1965;53:350–6.

[55] Yin X, Zhang Y, Guo S, Jin H, Wang W, Yang P. Large scale systematic proteomic quantification from non-metastatic to metastatic colorectal cancer. Sci Rep 2015;5:12120.

[56] An D, Wei X, Li H, Gu H, Huang T, Zhao G, et al. Identification of PCSK9 as a novel serum biomarker for the prenatal diagnosis of neural tube defects using iTRAQ quantitative proteomics. Sci Rep 2015;5:17559.

[57] Ademowo OS, Hernandez B, Collins E, Rooney C, Fearon U, van Kuijk AW, et al. Discovery and confirmation of a protein biomarker panel with potential to predict response to biological therapy in psoriatic arthritis. Ann Rheum Dis 2016;75:234–41.

[58] Tonry CL, Doherty D, OShea C, Morrissey B, Staunton L, Flatley B, et al. Discovery and Longitudinal Evaluation of Candidate Protein Biomarkers for Disease Recurrence in Prostate Cancer. J Proteome Res 2015;14:2769–83.

[59] Ramm S, Morissey B, Hernandez B, Rooney C, Pennington SR, Mally A. Application of a discovery to targeted LC-MS proteomics approach to identify deregulated proteins associated with idiosyncratic liver toxicity in a rat model of LPS/diclofenac co-administration. Toxicology 2015;331:100–11.

[60] Abraham SA, Hopcroft LEM, Carrick E, Drotar ME, Dunn K, Williamson AJK, et al. Dual

targeting of p53 and c-MYC selectively eliminates leukaemic stem cells. Nature 2016;534:341–6.

[61] Yang S, Zhang JJ, Huang XY. Orai1 and STIM1 Are Critical for Breast Tumor Cell Migration and Metastasis. Cancer Cell 2009;15:124–34.

[62] Schwarz G, Droogmans G, Nilius B. Multiple effects of SK&F 96365 on ionic currents and intracellular calcium in human endothelial cells. Cell Calcium 1994;15:45–54.

[63] Labelle D, Jumarie C, Moreau R. Capacitative calcium entry and proliferation of human osteoblast-like MG-63 cells. Cell Prolif 2007;40:866–84.

[64] Fowler T, Sen R, Roy AL. Regulation of Primary Response Genes. Mol Cell 2011;44:348–60.

[65] Iyer VR, Eisen MB, Ross DT, Schuler G, Moore T, Lee JC, et al. The transcriptional program in the response of human fibroblasts to serum. Science 1999;283:83–7.

[66] Reed SI. Ratchets and clocks: the cell cycle, ubiquitylation and protein turnover. Nat Rev Mol Cell Biol 2003;4:855–64.

[67] Rossman KL, Der CJ, Sondek J. GEF means go: turning on Rho GTPases with guanine nucleotide-exchange factors. Nat Rev Mol Cell Biol 2005;6:167–80.

[68] Ngok SP, Geyer R, Kourtidis A, Mitin N, Feathers R, Der CJ, et al. TEM4 is a junctional Rho GEF required for cell-cell adhesion, monolayer integrity and barrier function. J Cell Sci 2013;126:3271–7. doi:10.1242/jcs.123869.

[69] Madaule P, Furuyashiki T, Reid T, Ishizaki T, Watanabe G, Morii N, et al. A novel partner for the GTP-bound forms of rho and rac. FEBS Lett 1995;377:243–8.

[70] Cox-Paulson EA, Walck-Shannon E, Lynch AM, Yamashiro S, Zaidel-Bar R, Eno CC, et al. Tropomodulin protects ??-catenin-dependent junctional-actin networks under stress during epithelial morphogenesis. Curr Biol 2012;22:1500–5.

[71] Huang S, Chen CS, Ingber DE. Control of cyclin D1, p27(Kip1), and cell cycle progression in human capillary endothelial cells by cell shape and cytoskeletal tension. Mol Biol Cell 1998;9:3179–93.

[72] Hu W, Bellone CJ, Baldassare JJ. RhoA stimulates p27(Kip) degradation through its regulation of cyclin E/CDK2 activity. J Biol Chem 1999;274:3396–401.

[73] Monaco S, Rusciano MR, Maione AS, Soprano M, Gomathinayagam R, Todd LR, et al. A novel crosstalk between calcium/calmodulin kinases II and IV regulates cell proliferation in myeloid leukemia cells. Cell Signal 2015;27:204–14.

[74] El Boustany C, Bidaux G, Enfissi A, Delcourt P, Prevarskaya N, Capiod T. Capacitative calcium entry and transient receptor potential canonical 6 expression control human hepatoma cell proliferation. Hepatology 2008;47:2068–77.

[75] Chen Y-F, Chiu W-T, Chen Y-T, Lin P-Y, Huang H-J, Chou C-Y, et al. Calcium store sensor stromal-interaction molecule 1-dependent signaling plays an important role in cervical cancer growth, migration, and angiogenesis. Proc Natl Acad Sci U S A 2011;108:15225–30.

[76] Gao N, Zhang Z, Jiang B-H, Shi X. Role of PI3K/AKT/mTOR signaling in the cell cycle progression of human prostate cancer. Biochem Biophys Res Commun 2003;310:1124–32.

[77] Casagrande F, Bacqueville D, Pillaire MJ, Malecaze F, Manenti S, Breton-Douillon M, et al. G1 phase arrest by the phosphatidylinositol 3-kinase inhibitor LY 294002 is correlated to up-regulation of p27(Kip1) and inhibition of G1 CDKs in choroidal melanoma cells. FEBS Lett 1998;422:385–90.

[78] Zou Z-Q, Zhang X-H, Wang F, Shen Q-J, Xu J, Zhang L-N, et al. A novel dual PI3Kalpha/mTOR inhibitor PI-103 with high antitumor activity in non-small cell lung cancer cells. Int J Mol Med 2009;24:97–101.

[79] Wang Y-D, Su Y-J, Li J-Y, Yao X-C, Liang G-J. Rapamycin, a mTOR inhibitor, induced growth inhibition in retinoblastoma Y79 cell via down-regulation of Bmi-1. Int J Clin Exp Pathol 2015;8:5182–8.

[80] Olson MF, Ashworth a, Hall a. An essential role for Rho, Rac, and Cdc42 GTPases in cell cycle progression through G1. Science 1995;269:1270–2.

[81] Price LS, Leng J, Schwartz M a, Bokoch GM. Activation of Rac and Cdc42 by integrins mediates cell spreading. Mol Biol Cell 1998;9:1863–71.

[82] Olson MF, Ashworth a, Hall a. An essential role for Rho, Rac, and Cdc42 GTPases in cell cycle progression through G1. Science 1995;269:1270–2.

[83] Yang G, Thompson JA, Fang B, Liu J. Silencing of H-ras gene expression by retrovirus-mediated siRNA decreases transformation efficiency and tumorgrowth in a model of human ovarian cancer. Oncogene 2003;22:5694–701.

[84] Hurlin PJ, Fry DG, Maher VM, McCormick JJ. Morphological transformation, focus formation, and anchorage independence induced in diploid human fibroblasts by

expression of a transfected H-ras oncogene. Cancer Res 1987;47:5752–7.

[85] Taylor SJ, Shalloway D. Cell cycle-dependent activation of Ras. Curr Biol 1996;6:1621–7.

[86] Roovers K, Assoian RK. Integrating the MAP kinase signal into the G1 phase cell cycle machinery. Bioessays 2000;22:818–26.

[87] Murphy LO, Blenis J. MAPK signal specificity: the right place at the right time. Trends Biochem Sci 2006;31:268–75.

[88] Coleman ML, Marshall CJ, Olson MF. RAS and RHO GTPases in G1-phase cell-cycle regulation. Nat Rev Mol Cell Biol 2004;5:355–66.

[89] Mittnacht S, Paterson H, Olson MF, Marshall CJ. Ras signalling is required for inactivation of the tumour suppressor pRb cell-cycle control protein. vol. 7. 1997.

[90] Peeper DS, Upton TM, Ladha MH, Neuman E, Zalvide J, Bernards R, et al. Ras signalling linked to the cell-cycle machinery by the retinoblastoma protein. Nature 1997;386:177–81.

[91] Jiang K, Delarue FL, Sebti SM. EGFR, ErbB2 and Ras but not Src suppress RhoB expression while ectopic expression of RhoB antagonizes oncogene-mediated transformation. Oncogene 2004;23:1136–45.

[92] Vega FM, Colomba A, Reymond N, Thomas M, Ridley AJ. RhoB regulates cell migration through altered focal adhesion dynamics. Open Biol 2012;2:120076.

[93] Bousquet E, Mazières J, Privat M, Rizzati V, Casanova A, Ledoux A, et al. Loss of RhoB expression promotes migration and invasion of human bronchial cells via activation of

AKT1. Cancer Res 2009;69:6092–9.

[94] Sen A, O'Malley K, Wang Z, Raj G V, Defranco DB, Hammes SR. Paxillin regulates androgen- and epidermal growth factor-induced MAPK signaling and cell proliferation in prostate cancer cells. J Biol Chem 2010;285:28787–95.

[95] Qin J, Wang Z, Ma L, Ke J, Ni Q. Effects of paxillin on HCT-8 human colorectal cancer cells. Hepatogastroenterology 2011;58:1951–5.

AUTHOR CONTRIBUTIONS

Study concept and design: SRP. Acquisition of the data: AK, AvK and AI. Analysis and interpretation of the data: SRP and AK. Writing of the manuscript: SRP and AK.

ACKNOWLEDGMENT

AK was supported by a PhD studentship from the School of Medicine and Medical Sciences, University College Dublin; work in SRP's laboratory is supported by grants from Health Research Board [grant numbers HRA-POR-2015-1284 and HRA_POR/2011/125], Science Foundation Ireland, the Irish Cancer Society [grant number PCI11WAT], EU FP7 [grant number FP7-HEALTH-2012-INNOVATION-1-305266] and the Movember Global Action Plan [grant number 39231]. The UCD Conway Institute is funded by the Programme for Research in Third Level Institutions, as administered by the Higher Education Authority of Ireland.

Kieran Wynne of the UCD Conway Institute Mass Spectrometry Resource is acknowledged for expert technical advice and assistance with mass spectrometry. Alfonso Blanco of the UCD Conway Institute Flow Cytometry Core is acknowledged for expert assistance with flow cytometry. Amaya Garcia-Munoz and Javier Rodriguez are thanked for technical assistance. Claire Tonry, Angela Mc Ardle and Cinzia Raso are acknowledged for the proofreading of the manuscript.

CONFLICT OF INTEREST DISCLOSURE

The authors declare no competing financial interest.

ABBREVIATIONS:

CCE, capacitative calcium entry; CDK, cyclin-dependent kinases; CKI, cyclin dependent kinases inhibitors; EGF, epidermal growth factor; FASP, filter aided sample preparation; FDR, false discovery rate; IPA, Ingenuity Pathway Analysis; MS/MS, tandem mass spectrometry; nLC, nano Liquid Chromatography; R point, restriction point late in G_1 phase; Rb, Retinoblastoma protein; SK&F96365, selective inhibitor of CCE (1-[2-(4-Methoxyphenyl)-2-[3-(4-methoxyphenyl)propoxy]ethyl-1H-imidazole hydrochloride).

Table 1. List of 10 most down-regulated and up-regulated proteins identified in cells with inhibited Ca^{2+} influx. Protein ID, protein name, gene name, log_2 fold change, and p-value is listed for each protein.

Protein IDs	Protein names	Gene names	Log_2 fold change G+/G	t-test p-value G+/G
Top ten down-regulated proteins				
P26232	Catenin alpha-2	CTNNA2	-26.40	8.85E-06
Q5VST9	Obscurin	OBSCN	-25.01	2.56E-08
P36021	Monocarboxylate transporter 8	SLC16A2	-23.92	1.81E-06
Q58DX5	Inactive N-acetylated-alpha-linked acidic dipeptidase-like protein 2	NAALADL2	-23.87	3.94E-06
Q96EY5	Multivesicular body subunit 12A	MVB12A	-23.67	1.05E-06
Q9H3M7	Thioredoxin-interacting protein	TXNIP	-2.20	6.74E-03
Q96A35	39S ribosomal protein L24, mitochondrial	MRPL24	-1.89	2.41E-02
Q5J8M3	ER membrane protein complex subunit 4	EMC4	-1.77	3.96E-02
Q9NSK7	Protein C19orf12	C19orf12	-1.52	1.78E-02
Q9BVL4	Selenoprotein O	SELO	-1.44	3.63E-02
Top ten up-regulated proteins				
Q9NXS2	Glutaminyl-peptide cyclotransferase-like protein	QPCTL	25.28	3.77E-09
Q8WU79	Stromal membrane-associated protein 2	SMAP2	24.67	1.01E-07
Q96PE2	Rho guanine nucleotide exchange factor 17	ARHGEF17	23.95	2.72E-07
Q7Z6K3	Protein prenyltransferase alpha subunit repeat-containing protein 1	PTAR1	21.87	2.12E-07
Q12789	General transcription factor 3C polypeptide 1	GTF3C1	4.03	3.91E-02
P53539	Protein fosB	FOSB	3.54	2.62E-04
Q9UHA3	Probable ribosome biogenesis protein RLP24	RSL24D1	2.29	1.81E-02
Q96EC8	Protein YIPF6	YIPF6	2.00	3.67E-03
Q5MNZ9	WD repeat domain phosphoinositide-interacting protein 1	WIPI1	1.72	1.99E-02

O60238	BCL2/adenovirus E1B 19 kDa protein-interacting protein 3-like	BNIP3L	1.56	3.19E-02

Table 2. List of proteins selected by heat map analysis. Protein ID, protein name, gene name and p-value is listed for each protein.

Protein ID	Protein name	Gene name	ANOVA p-value
Q96PE2	Rho guanine nucleotide exchange factor 17	ARHGEF17	2.89E-12
Q7Z6K3	Protein prenyltransferase alpha subunit repeat-containing protein 1	PTAR1	5.22E-12
O95163	Elongator complex protein 1	IKBKAP	1.80E-03
Q5T1M5	FK506-binding protein 15	FKBP15	3.54E-02
Q9Y2S2	Lambda-crystallin homolog	CRYL1	3.46E-02
Q9NZR1	Tropomodulin-2	TMOD2	4.45E-02
Q8NHZ8	Anaphase-promoting complex subunit CDC26	CDC26	4.47E-02
O60238	BCL2/adenovirus E1B 19 kDa protein-interacting protein 3-like	BNIP3L	4.05E-02
Q96GK7	Fumarylacetoacetate hydrolase domain-containing protein 2A;Fumarylacetoacetate hydrolase domain-containing protein 2B	FAHD2A;FAHD2B	4.64E-02
Q9NS86	LanC-like protein 2	LANCL2	2.93E-02
P98194	Calcium-transporting ATPase type 2C member 1	ATP2C1	3.98E-02
Q92759	General transcription factor IIH subunit 4	GTF2H4	4.59E-02
Q12789	General transcription factor 3C polypeptide 1	GTF3C1	3.67E-02
Q16611	Bcl-2 homologous antagonist/killer	BAK1	4.35E-02
Q9NP66	High mobility group protein 20A	HMG20A	4.52E-02
O14578	Citron Rho-interacting kinase	CIT	4.82E-02
Q9UQ13	Leucine-rich repeat protein SHOC-2	SHOC2	5.55E-03
Q96B26	Exosome complex component RRP43	EXOSC8	4.24E-02
P49815	Tuberin	TSC2	8.49E-03
Q96J02	E3 ubiquitin-protein ligase Itchy homolog	ITCH	4.93E-02
O95989	Diphosphoinositol polyphosphate phosphohydrolase 1	NUDT3	4.14E-02
Q99622	Protein C10	C12orf57	1.44E-02

Table 3. List of proteins selected by PCA. Protein ID, protein name, gene name, rank order and p-value is listed for each protein.

Protein IDs	Protein names	Gene names	Rank order	ANOVA p-value
Q9NXS2	Glutaminyl-peptide cyclotransferase-like protein	QPCTL	1	4.31E-03
P22736	Nuclear receptor subfamily 4 group A member 1	NR4A1	2	6.32E-03
Q9Y241	HIG1 domain family member 1A, mitochondrial	HIGD1A	3	8.20E-03
Q86U86	Protein polybromo-1	PBRM1	4	3.13E-12
Q96PE2	Rho guanine nucleotide exchange factor 17	ARHGEF17	5	2.89E-12
Q12789	General transcription factor 3C polypeptide 1	GTF3C1	6	3.67E-02
Q7Z6K3	Protein prenyltransferase alpha subunit repeat-containing protein 1	PTAR1	7	5.22E-12
O14578	Citron Rho-interacting kinase	CIT	8	4.82E-02
Q9NP66	High mobility group protein 20A	HMG20A	9	4.52E-02
Q16611	Bcl-2 homologous antagonist/killer	BAK1	10	4.35E-02
Q92759	General transcription factor IIH subunit 4	GTF2H4	11	4.59E-02
Q6PML9	Zinc transporter 9	SLC30A9	12	3.05E-12
Q5JTD0	Tight junction-associated protein 1	TJAP1	13	1.60E-11
Q9NZR1	Tropomodulin-2	TMOD2	14	4.45E-02
Q9Y2S2	Lambda-crystallin homolog	CRYL1	15	3.46E-02
P55210	Caspase-7;Caspase-7 subunit p20;Caspase-7 subunit p11	CASP7	16	1.73E-12
O60238	BCL2/adenovirus E1B 19 kDa protein-interacting protein 3-like	BNIP3L	17	4.05E-02
Q8NHZ8	Anaphase-promoting complex subunit CDC26	CDC26	18	4.47E-02
P25205	DNA replication licensing factor MCM3	MCM3	19	6.17E-03
Q96B26	Exosome complex component RRP43	EXOSC8	20	4.24E-02
Q9BZE9	Tether containing UBX domain for GLUT4	ASPSCR1	21	3.56E-02
Q86U44	N6-adenosine-methyltransferase 70 kDa subunit	METTL3	22	4.65E-03
Q9NWU5	39S ribosomal protein L22, mitochondrial	MRPL22	23	1.00E-02
P19022	Cadherin-2	CDH2	24	8.13E-03
Q9Y2P8	RNA 3-terminal phosphate cyclase-like protein	RCL1	25	8.59E-03

O15083	ERC protein 2	ERC2	26	7.05E-03
P29279	Connective tissue growth factor	CTGF	27	2.80E-03
O00622	Protein CYR61	CYR61	28	1.64E-03
O95870	Abhydrolase domain-containing protein 16A	ABHD16A	29	9.63E-03

Table 4. List of biological processes associated with 182 proteins that were found to be differentially expressed in cells with inhibited Ca^{2+} influx. Categories, functional annotation, p-value, activation z-score, molecules and number of molecules is listed for each biological process.

Categories	Functions Annotation	p-value	Activation z-score	Molecules	# Molecules
Protein Degradation, Protein Synthesis	catabolism of protein	1.51E-06	0	ATG4B,EGFR,NEDD8,PSMB3, PSMD14,PSMF1,UBE2D2,UBE2D3, UBE2K,UCHL1	10
RNA Post-Transcriptional Modification	splicing of RNA	2.15E-06	-1.34	CDC42,EPB41,HNRNPH3,LUC7L3, PPIH,SAP18,SNRPD1,SNRPF,SRSF9	9
Cellular Assembly and Organization	development of cytoplasm	3.07E-06	-1.93	ABCD1,ARHGEF17,ATG4B,CDC42, CDK4,EGFR,F2R,HRAS,IKBKB,IPO9, MAP1B,PXN,RHOB,TBCD,TBCE,VPS4A	16
Protein Degradation, Protein Synthesis	degradation of protein	4.09E-06	0	ATG4B,EGFR,IKBKB,IPO9,NCKAP1, NEDD8,PIK3R1,PSMB3,PSMD14, PSMD2,PSMF1,TSG101,UBE2D2, UBE2D3,UBE2K,UCHL1,UFSP2,VPS4A	18
Protein Synthesis	metabolism of protein	9.12E-06	-0.66	ATG4B,CDK4,EGFR,EIF3I,GPC1,IKBKB, IPO9,NCKAP1,NEDD8,PIK3R1,PSMB3, PSMD14,PSMD2,PSMF1,RPL19,TSC2, TSG101,UBE2D2,UBE2D3,UBE2K, UCHL1,UFSP2,UPF1,VPS4A	24
Cellular Movement	cell movement of fibroblast cell lines	1.05E-05	-0.34	ACP1,ADI1,CDC42,EGFR,ERBB4, GPC1,HRAS,PIK3R1,PXN	9
Cellular Growth and Proliferation	proliferation of fibroblast cell lines	1.24E-05	-0.21	ACP1,CDC42,CDK4,EEF1D,EGFR, EIF3I,ERBB4,F2R,HRAS,IKBKB, PIK3R1,RHOB,TSC2,TSNAX,TXNIP	15
Cell Morphology	shape change of fibroblasts	2.09E-05	-0.42	CDC42,HRAS,PXN,RHOB,TSC2	5
RNA Post-Transcriptional Modification	processing of RNA	3.41E-05	-1.342	CDC42,EPB41,HNRNPH3,LUC7L3, PPIH,SAP18,SNRPD1,SNRPF,SRSF9, UPF1,WDR43	11
Cellular Growth and Proliferation	colony formation of fibroblast cell lines	1.02E-04	0.26	CDC42,EGFR,ERBB4,HRAS,RHOB, TSC2	6
Cellular Assembly and Organization	formation of cytoskeleton	1.13E-04	-2.11	ARHGEF17,CDC42,CDK4,EGFR,F2R, HRAS,IKBKB,MAP1B,PXN,RHOB, TBCD,TBCE	12
Cellular Assembly and Organization	quantity of filaments	1.19E-04	-0.34	CDC42,EPB41,HRAS,MAP1B,RHOB, RHOJ,TBCE	7
Cell Morphology	cell spreading of tumor cell lines	1.36E-04	-1.34	CDC42,EGFR,HRAS,PXN,RAP2B, UCHL1	6

Cellular Assembly and Organization	formation of actin stress fibers	1.81E-04	-2.41	ARHGEF17,CDC42,CDK4,EGFR,F2R, HRAS,IKBKB,PXN,RHOB	9
Cell Death and Survival	apoptosis of fibroblast cell lines	2.22E-04	-0.34	CDK4,EGFR,EIF3I,ERBB4,HRAS,IKBKB, MAPKAP1,PIK3R1,RHOB,TSC2,TXNIP	11
Cellular Assembly and Organization	formation of filaments	3.19E-04	-2.11	ARHGEF17,CDC42,CDK4,EGFR,F2R, HRAS,IKBKB,MAP1B,PXN,RHOB,TBCD, TBCE	12
Cellular Assembly and Organization	retraction of cellular protrusions	4.38E-04	-0.28	CDC42,CDC42BPA,F2R,HRAS,MAP1B	5
Cellular Growth and Proliferation	arrest in proliferation of cells	5.86E-04	0	AKT3,CDC42,CDK4,EGFR,HRAS,IKBKB, TSG101,UBE2D3	8
Molecular Transport	transport of molecule	5.96E-04	-1.36	ABCD1,AGK,AKT3,ARFIP1,CDC42,CDK4, CHMP3,ENSA,ERBB4,F2R,GAR1,HRAS, IKBKB,IPO9,MAP1B,MAPKAP1,PHAX, PIK3R1,PKN1,RHOB,SLC16A2,SLC25A20, SLC33A1,TSC2,TSG101,TSNAX,TXNIP, UPF1,VPS4A	29
RNA Post-Transcriptional Modification	splicing of mRNA	7.10E-04		HNRNPH3,PPIH,SAP18,SNRPD1,SRSF9	5
Molecular Transport	transport of protein	8.06E-04	0	ARFIP1,CHMP3,IPO9,MAP1B,RHOB, TSC2,TSG101,TSNAX,TXNIP	9
Cell Morphology	cell spreading	9.01E-04	-0.56	ACP1,CDC42,EGFR,HRAS,IPO9,PXN, RAP2B,RHOB,UCHL1	9
Cell Morphology	reorganization of cytoskeleton	1.05E-03	-1.18	CDC42,CDC42BPA,EGFR,F2R,HRAS, PXN,RHOB	7
Cell Death and Survival	apoptosis of ovarian cancer cell lines	1.09E-03	-1.98	EGFR,ERBB4,HRAS,IKBKB,TSG101	5
Cell Death and Survival	cell death of fibroblasts	1.74E-03	-0.94	CDC42,EGFR,HRAS,IKBKB,RHOB, TSC2,TSG101,UBE2K	8
Cell Morphology	formation of lamellipodia	1.93E-03	-0.60	CDC42,EGFR,HRAS,NCKAP1, PXN,RHOB	6
DNA Replication, Recombination, and Repair	synthesis of DNA	2.04E-03	-1.36	CDC42,CDK4,EGFR,ERBB4,F2R,HRAS, IKBKAP,PIK3R1,PXN,TSC2,WDR11	11
Cellular Assembly and Organization	organization of actin cytoskeleton	2.83E-03	0	ARHGEF17,CDC42,CDC42BPA,EGFR, EPB41,HRAS,RHOB,RHOJ	8
Cell Death and Survival	cell death	3.88E-03	-0.80	ABCD1,ACP1,ADI1,AKT3,BRCC3,CBR1, CDC42,CDK4,CHMP3,CTNNA2,DDX19A, EEF1D,EGFR,EIF3I,EPB41,ERBB4,F2R, FAHD2A,GPC1,HRAS,IKBKAP,IKBKB, MAP1B,MAPKAP1,MCM2,MSI1,MSI2, NCKAP1,NEDD8,NLE1,OBSCN,PIGT, PIK3R1,PKN1,PSMD14,PSMD2,PUM1, PXN,RGS10,RHOB,RHOJ,SAP18, ST3GAL1,TBCE,TSC2,TSG101,TXNIP, UBE2K,UCHL1,UPF1	50
Cellular Movement	cell movement of fibroblasts	4.40E-03	-2.40	CDC42,F2R,HRAS,IKBKB,PXN,RHOB	6
Cellular Assembly and Organization	organization of cytoplasm	4.69E-03	-0.24	ABCD1,ACP1,ARFGEF1,ARHGEF17, BCS1L,CDC42,CDC42BPA,CTNNA2, EGFR,EPB41,ERBB4,F2R,HRAS,IKBKB, KIF3B,MAP1B,NCKAP1,PIK3R1,PXN, RHOB,RHOJ,TBCD,TBCE,UCHL1	24

Cell-To-Cell Signaling and Interaction	attachment of cells	5.39E-03	0.11	ACP1,EGFR,HRAS,IPO9,RHOB	5
Cellular Assembly and Organization	formation of focal adhesions	5.71E-03		CDC42,CDC42BPA,HRAS,PXN,RHOB	5
Cell Death and Survival	apoptosis of fibroblasts	7.98E-03	-0.22	CDC42,EGFR,HRAS,IKBKB,RHOB,TSC2	6
Cell Morphology	neuritogenesis	7.99E-03	1.57	CDC42,CTNNA2,EGFR,ERBB4,HRAS, KIF3B,MAP1B,PXN,RHOB,TBCE,UCHL1	11
Cell Morphology	branching of neurites	9.50E-03	1.67	CDC42,CTNNA2,ERBB4,HRAS, KIF3B,MAP1B,RHOB	7
Cellular Assembly and Organization	microtubule dynamics	1.12E-02	0.08	ACP1,CDC42,CDC42BPA,CTNNA2, EGFR,EPB41,ERBB4,F2R,HRAS,IKBKB, KIF3B,MAP1B,NCKAP1,PIK3R1, PXN,RHOB,TBCD,TBCE,UCHL1	19
Molecular Transport	localization of protein	1.20E-02		CDC42,NCKAP1,NEDD8,PIK3R1,TSC2	5
Cellular Growth and Proliferation	colony formation	1.21E-02	-0.52	CDC42,EGFR,EPB41L3,ERBB4,HRAS, IKBKB,PBXIP1,PIK3R1,PXN,RHOB,TSC2	11
Cell Morphology	formation of cellular protrusions	1.25E-02	1.03	ACP1,CDC42,CDC42BPA,CTNNA2, EGFR,ERBB4,HRAS,IKBKB,KIF3B, MAP1B,NCKAP1,PXN,RHOB,TBCE, UCHL1	15
Cellular Growth and Proliferation	proliferation of fibroblasts	1.42E-02	-0.50	ACP1,CDK4,EGFR,HRAS,IKBKB, TSC2,TSG101,TXNIP	8
Cellular Assembly and Organization	organization of cytoskeleton	1.43E-02	-0.24	ACP1,ARHGEF17,CDC42,CDC42BPA, CTNNA2,EGFR,EPB41,ERBB4,F2R, HRAS,IKBKB,KIF3B,MAP1B,NCKAP1, PIK3R1,PXN,RHOB,RHOJ,TBCD,TBCE, UCHL1	21
Cell Cycle	mitogenesis	1.47E-02	0.85	EGFR,ERBB4,HRAS,IKBKB,PIK3R1	5

FIGURE CAPTIONS

Figure 1. An effect of SK&F96365 on Ca^{2+} influx and cell cycle progression. [A] Typical cytoplasmic Ca^{2+} traces of quiescent MRC-5 cells stimulated with serum growth factors in the presence and absence of Ca^{2+} influx inhibitor, SK&F96365. Ca^{2+} traces represent an average 340/380 ratio of Fura-2 acquired from single cells in a single experiment (approximately n = 10 cells). Figure is a representative figure of five independent experiments. [B] Effect of SK&F96365 on the distribution of cells at distinct phases of cell cycle upon stimulation of quiescent cells with serum growth factors. MRC-5 cells stimulated with serum growth factors in the absence and presence of SK&F96365 were stopped 20 h after stimulation, fixed and stained with PI. An intensity of PI was acquired by flow cytometry. Data are an average ± SD of three independent experiments. [C] Dose response effect of SK&F96365 on entry of MRC-5 cell to S phase. Quiescent MRC-5 cells stimulated with serum growth factors in the presence of increasing amounts of SK&F96365. Cells were stopped 20 h after treatment and % of the cells in S phase was evaluated by flow cytometry analysis of PI staining of fixed cells. Data are an average ± SD of three independent experiments. [D] Effect of SK&F96365 on cell cycle progression upon stimulation of quiescent cells with serum growth factors. Quiescent cells were loaded with CFSE and then stimulated with serum growth factors in the absence and presence of SK&F96365 to monitor an effect of inhibition of Ca^{2+} influx on cell proliferation. CFSE intensity was analysed 48 h after stimulation by flow cytometry. Data are an average ± SEM of three independent experiments.

Figure 2. Schematic illustration of sample preparation and analysis of label-free discovery experiment. Three biological replicates of MRC-5 cells of four treatment conditions C, C+, G

and G+ were lysed in SDS based lysis buffer and protein concentration was determined with BCA assay. The lysates were digested according to FASP procedure. Peptides were quantified with NanoDrop and then desalted on StageTips prior to analysis on Q-Exactive. Each biological replicate was analysed in two technical replicates on the Q-Exactive. Quality of data from nLC-MS/MS analysis was visually inspected with Xcalibur™. Proteins were identified and quantified in MaxQuant and the selection of statistically important proteins was performed in Perseus. Biological importance of the data was analysed with IPA. Selected findings were validated by functional assays and Western blot analysis.

Figure 3. Representative illustration of the quality of nLC-MS/MS data. Representative total ion current (TIC) chromatograms of summed intensities detected from nLC-MS/MS analysis of control samples at each time point. TICs show an analysis of MRC-5 whole cell digest of [A] technical and [B] biological replicates. The x-axis represents the time of acquisition and the y-axis relative abundance of the ions. Dot plots show the correlation between LFQ intensities of [C] technical and [D] biological replicates of control samples and the numbers represent the Pearson's correlation values for each dot plot. Venn diagrams of proteins identified in MRC-5 cell lysates are shown. [E] Comparison of the total number of proteins identified in two technical replicates of control cells and [F] the overlap of number of proteins identified in three biological replicates of control cells indicates excellent experimental reproducibility.

Figure 4. Effect of Ca^{2+} influx on protein expression during cell cycle initiation and progression. [A] Volcano plot showing protein expression changes in MRC-5 cells stimulated with growth factors in the presence of SK&F96365. □ indicates proteins that significantly change at $p < 0.05$ [B] Unsupervised hierarchical clustering was performed on protein

expression profiles of three biological replicates of control cells (C), control cells treated with SK&F96365 (C+), cells stimulated with mixture of growth factors (G) and cells stimulated with mixture of growth factors in the presence of SK&F96365 (G+) differentially expressed between investigated conditions. The heat map of 291 proteins differentially expressed proteins based on clustering are shown in this figure. Each column represents a different treatment condition plotted as a three biological replicates and each row represents a proteins. Blue indicates proteins that were up-regulated and yellow indicates proteins that were down-regulated. Black shows proteins whose expression is unchanged between investigated conditions. [C] Principal Component Analysis (PCA) of control (C), control cell in the presence of SK&F96365 (C+), growth factors (G) and growth factors in the presence of SK&F96365 (G+).

Figure 5. Venn diagrams summarising protein overlap between proliferation, morphology and assembly and organisation. 182 proteins were uploaded to IPA and based on the Ingenuity database mapped to the biological processes. Venn diagram shows an overlap of proteins regulated by Ca^{2+} inhibition and associated with cell proliferation, morphology and cellular assembly and organisation. Proteins indicated with ★ were selected for further validation by WB.

Figure 6. Western blot validation of label-free nLC-MS/MS data. Proteins from cell lysates of four treatment conditions C, C+, G, G+ were separated on 1D-gel and then transferred on PVDF membrane. Detection of the protein was performed with specific for proteins primary antibodies. Figure shows representative Western blot images of three independent experiments for [A] paxillin, [C] RAS and [E] CDC42. GAPDH was used as loading control. Relative density analysis of the [B] paxillin, [D] RAS and [F] CDC42 protein bands between

cell treated with growth factors in the absence (G) and presence of SK&F96365 (G+). GAPDH was used as the internal control in relative density analysis. Values are averages from three independent experiments. Each value is expressed as mean ± SD. *** $p < 0.001$, G vs G+ group.

Figure 7. **Possible mechanism of CCE dependent regulation of cell cycle in [A] the presence and [B] absence of Ca^{2+} ions.**

Figure 1

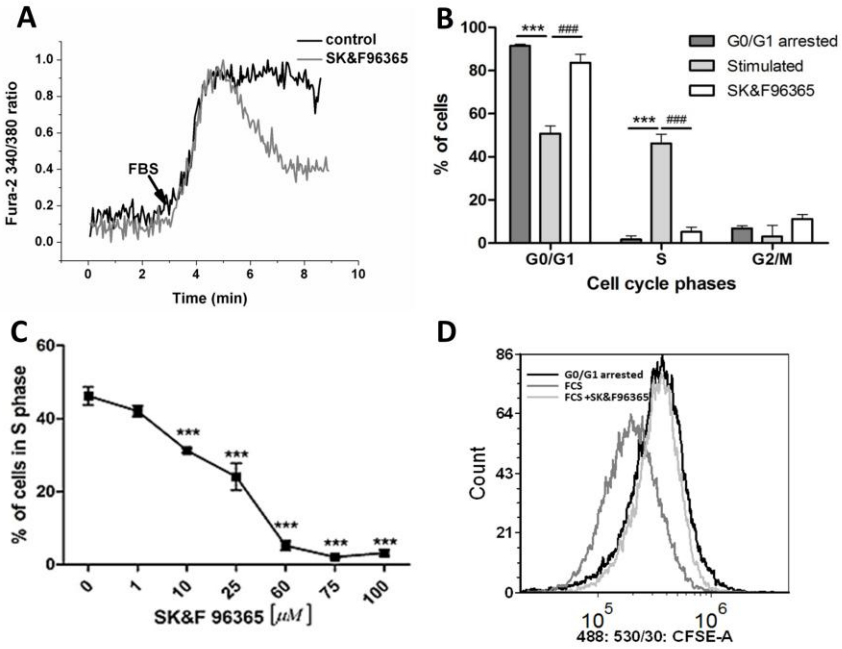

Figure 2

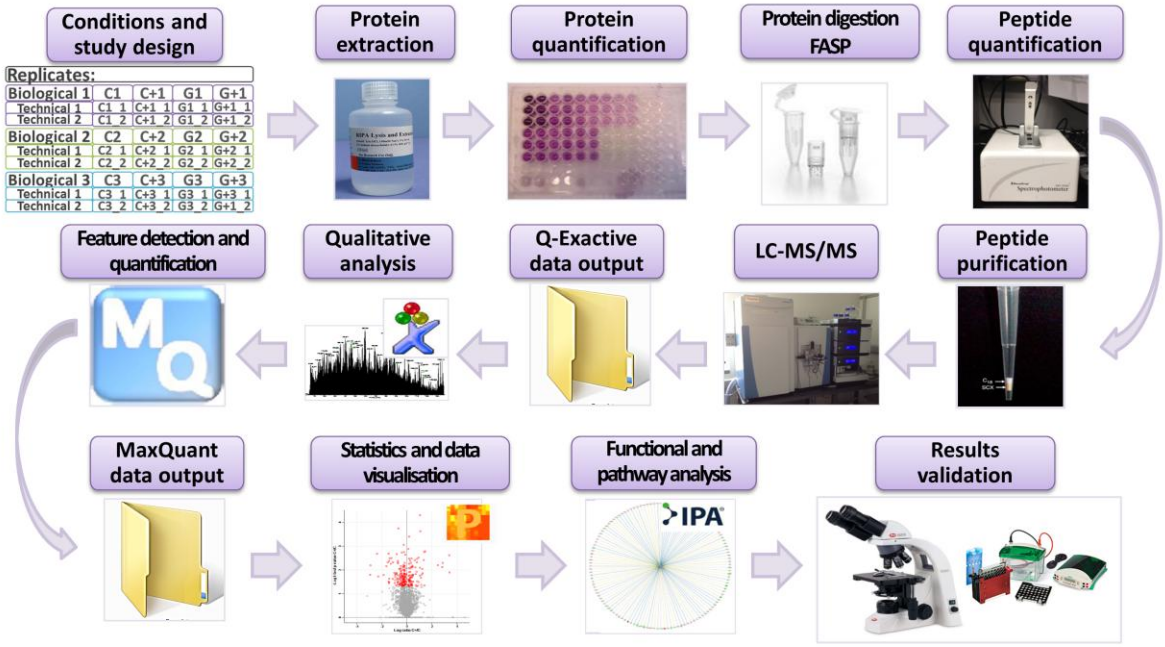

Figure 3

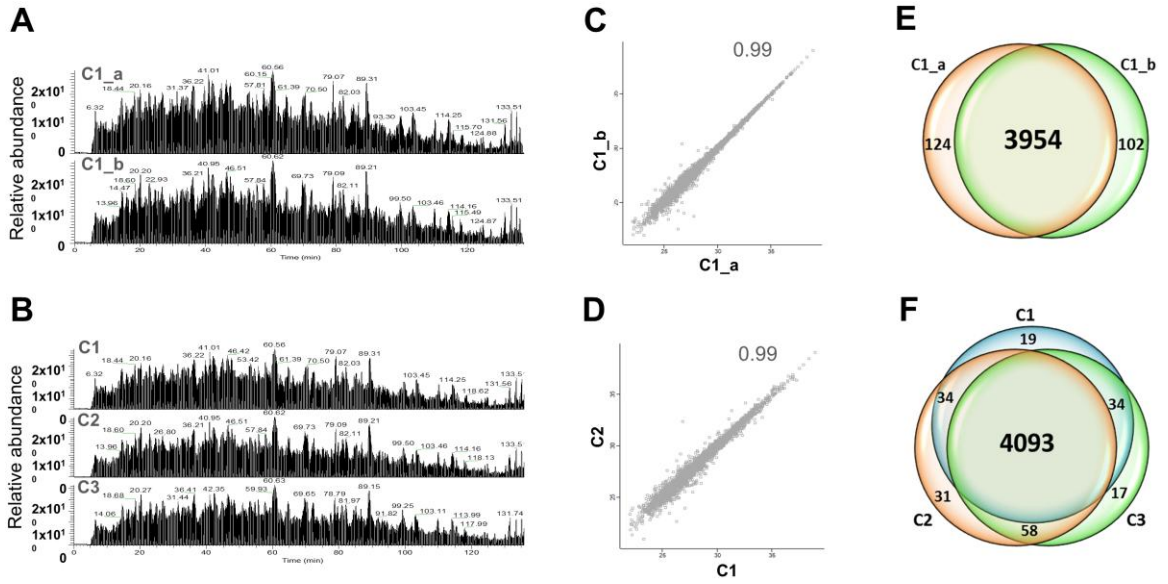

Figure 4

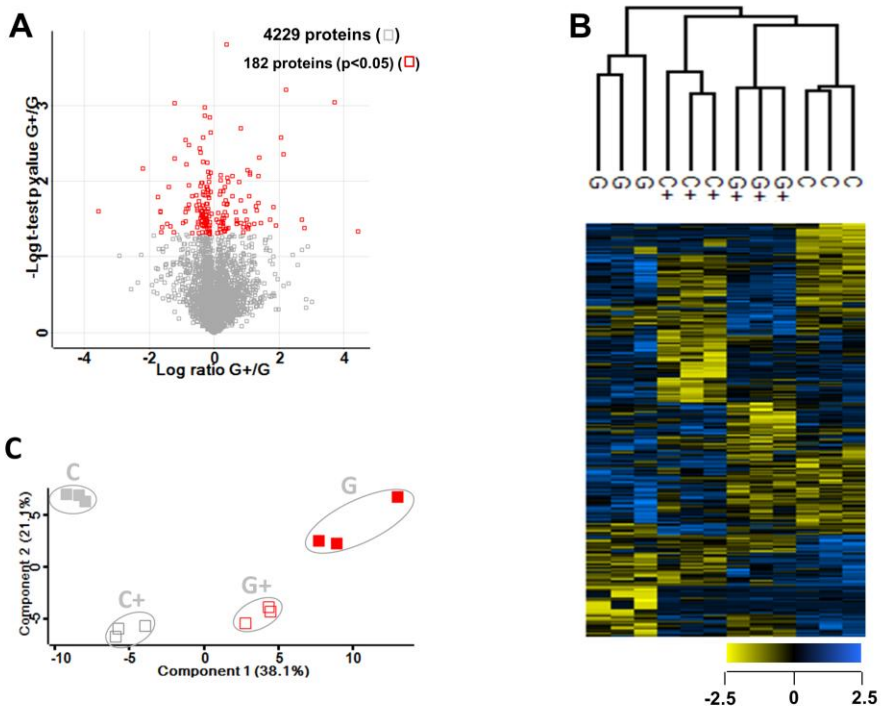

Figure 5

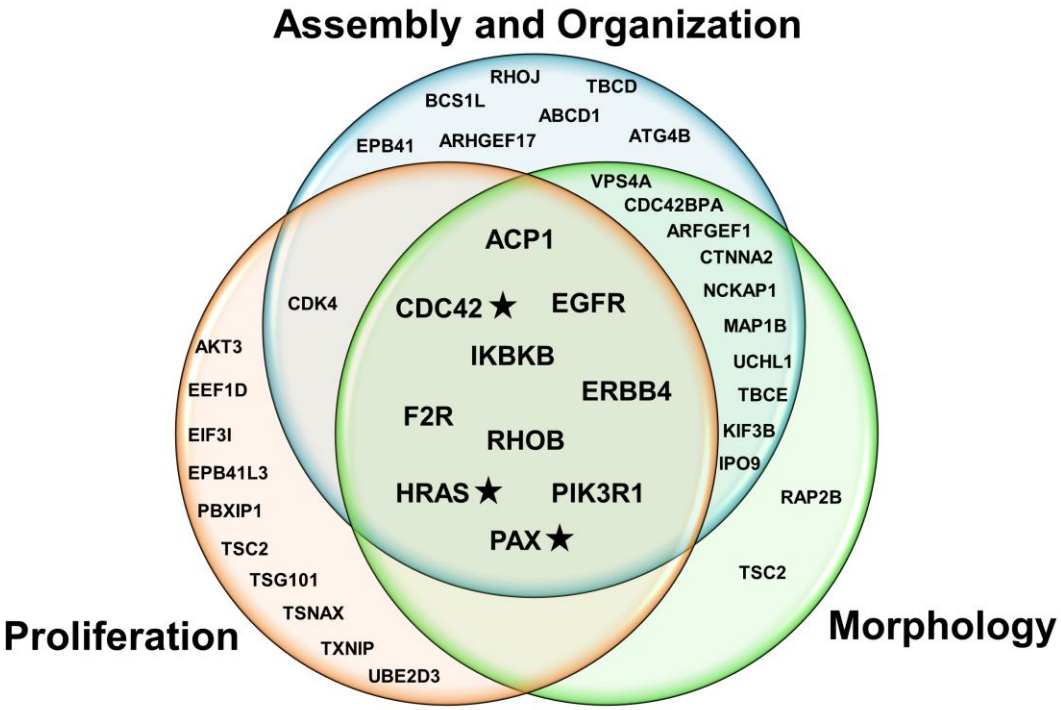

Figure 6

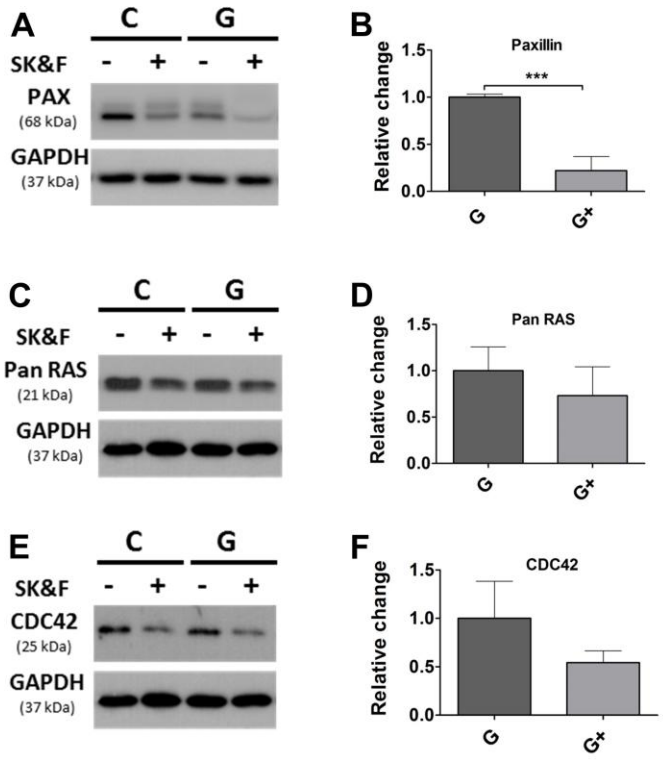

Figure 7

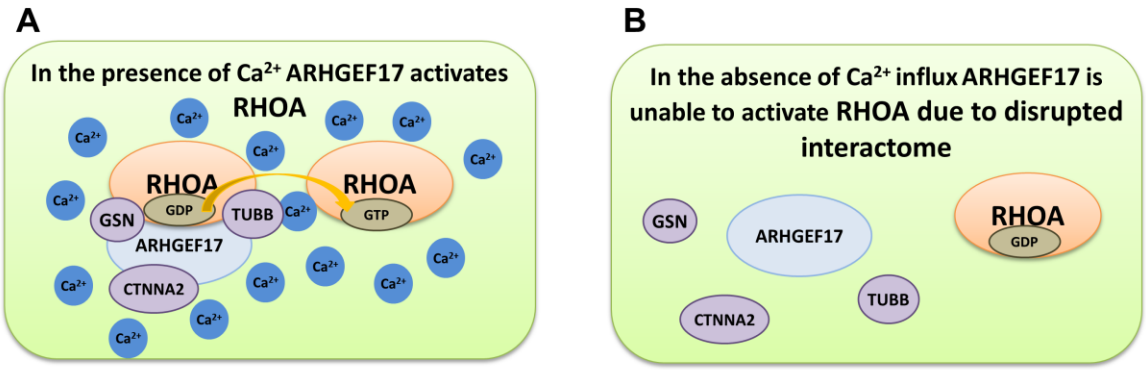

Biological Significance

The results of this study provide new insight into Ca^{2+} dependent regulation of cell cycle. This manuscript reports first to date global analysis of Ca^{2+} regulated protein expression changes early in G_1 in non-transformed human fibroblast cell line. It also highlights cannonical signaling pathways and biological processes that are regulated by the inhibition of Ca^{2+} influx. Importantly, it appears that Ca^{2+} may be the factor that links cell division with enviromental cues, cell morphology and cellular assembly and organization, on which cell proliferation depends. Hence, the findings presented here provide numerous opportunities for more detailed investigations of the mechanism of Ca^{2+} dependent regulation of cell cycle at the molecular and systemic level.

Graphical Abstract